Master's Thesis

Beam Loading Studies for Cavity Phase and Amplitude Setting

Staffan Rydén

Department of Electrical and Information Technology,
Faculty of Engineering, LTH, Lund University, May 2015.

Beam Loading Studies for Cavity Phase and Amplitude Setting

Staffan Rydén

Department of Electrical and Information Technology
Lund University

Advisor:
Rihua Zeng
Hooman Hassanzadegan

May 18, 2015

Printed in Sweden
E-huset, Lund, 2015

Abstract

The purpose of this thesis is to study beam-cavity interactions, with a focus on how to maintain an unperturbed acceleration field in a conducting cavity with a proton beam present. The impact on a cavity acceleration field from different perturbation sources is investigated through computer simulations of a theoretical model based on a resonant circuit. Perturbations from the RF input pulse to the cavity, from the cavity field control system and from the proton beam pulse shape are investigated.

The cavity field control system is dependent on accurate measurement of the beam phase and accelerator operation requires accurate measurements of the beam position. Therefore the thesis also aims to analyze the limitations of beam position monitors (BPMs) in detecting the phase and position of the proton beam, and to analyze and identify relative performance degradation of beam phase detection when measuring a low current beam with varying pulse length. This is done through measurements on a scale model of a pipe section with BPMs.

The theory section gives an overview of the cavity model, cavity beam loading, beam position monitoring and phase scan theory. RF input pulses that generates the required cavity field while fulfilling cavity perturbation criteria are identified. Finally the thesis attempts to improve linear accelerator performance by finding RF input pulses and cavity settings that minimize energy consumption while also fulfilling the requirements for cavity field stability and BPM accuracy.

Table of Contents

List of Figures

List of Tables

Chapter 1

Introduction

The European Spallation Source, ESS, is a particle accelerator currently under construction in Lund, Sweden, that aims to provide a flexible source of neutrons for research purposes. Since neutrons are uncharged particles they cannot be accelerated directly but are instead produced by accelerating protons, by means of a linear accelerator, and colliding them with a tungsten target. The neutron energy is dependent on the energy of the protons hitting the tungsten target. To make the target last longer the beam is swept across the target in a raster pattern, evenly exposing a larger area of the target.

In order to accelerate protons in a controlled manner it is crucial to provide a constant electric field strength in the accelerating cavities, compensating for perturbations to the field caused by the passing proton beam. It is also vital to be able to accurately measure the beam position and phase. The beam phase measurement is crucial to the cavity control system and the beam position is needed in order to sweep the beam correctly across the target and avoid scenarios where the beam is misdirected and damages the accelerator equipment.

One important factor in these problems is the properties of the proton beam. The proton beam consists of *bunches* of protons that travel in sequence through the accelerating cavities of the linear accelerator. The proton beam is a *pulsed* beam, with each pulse consisting of a multitude of proton bunches. The *shape* of these proton beam pulses, namely the beam pulse current and the beam pulse length, affect both the perturbations to the cavity as well as the ability of the beam position monitoring system to measure the beam position.

Another important issue is to set the correct phase and amplitude for the cavities to ensure that the proton bunches receive the desired acceleration, i.e. energy gain, at each cavity. The most common methods to set amplitude and phase for proton linear accelerators are *time of flight* measurements and so called *phase scan* methods. Phase scan methods here refers to the way of calibrating setting points for RF cavities by scanning RF phase, measuring beam arrival time at downstream locations, comparing the measured data to model predicted data, and identifying the best-matched data for calibration.

Two examples of classical phase scan methods are the ΔT method and the phase signature method which are used widely in existing normal conducting linear accelerators such as in LAMPF, Fermilab, JPARC and SNS. See [1] for more detailed information about phase scan methods.

The phase scan is performed using a beam consisting of very short pulses with low current while downstream sections of the linear accelerator are unpowered resulting in a severely de-bunched low current beam. This poses a particularly challenging scenario for beam position monitoring.

Before inserting the proton beam into the cavity the cavity field must be charged up to the desired electric field strength. This is referred to as *cavity filling*. The power consumed during filling and the speed required for it depends on the RF input pulse shape.

The main purpose of this thesis is to study the impact of different beam pulse shapes on cavity perturbation and beam position monitoring. Cavity perturbation using different error correction control systems is investigated and the optimization of cavity parameters is explained. The thesis also contains a study of cavity filling for different RF input pulse shapes.

Since the cavity field control system relies on accurate measurements of beam phase to function properly and the accelerator could be damaged by a misdirected beam it is vital that the beam position monitor, BPM, system is able to accurately measure the beam position and phase. Therefore the thesis also investigates the capabilities of the BPM system.

Cavity perturbation studies are made using an existing MATLAB simulink model of a cavity, created by Rihua Zeng, which is based on a resonant circuit model. Evaluation of BPM ability is done through measurements on an existing physical scale model of a pipe section of the linear accelerator, designed by Hooman Hassanzadegan.

Chapter 2

Background

2.1 The need for neutron science

Neutron scattering techniques are non-destructive imaging techniques providing a combination of high sensitivity and high penetration that allows monitoring of structures and motions on a molecular level. Because of these unique properties the techniques have applications in many scientific disciplines including physics, chemistry, biology, materials science, engineering and archaeology. Using neutrons it is possible to probe magnetism and superconductivity and study the molecular structure of experimental materials as well as old artifacts.

Neutron scattering is used a compliment to other techniques such as electron scattering and synchrotron light x-ray radiation. While electrons provide unparalleled resolution of structures they have poor penetration. Synchrotron light x-ray radiation has good penetration but is not as good for imaging for example plastics, ceramics and fluids as neutron scattering is since x-rays easily penetrates those materials.

2.2 ESS - European Spallation Source

The European Spallation Source (ESS) is a neutron source currently under construction in Lund, Sweden. The ESS facility is designed to provide a flexible source of neutrons for research purposes. It is scheduled to produce its first neutrons in 2019.

The neutrons will be produced by shooting a beam of high energy protons at a tungsten target, which will then emit high energy neutrons. A linear accelerator, *linac*, will be used to accelerate a pulsed proton beam with an average current of 62.5 mA, a pulse length of 2.86 ms, and a repetition rate of 14 Hz, from 75 keV to 2.0 GV by a series of radio frequency (RF) accelerating cavities such as RFQ, DTL, spoke and elliptical superconducting cavities, see figure 2.1. The total number of accelerating cavities is 155 in the current design.

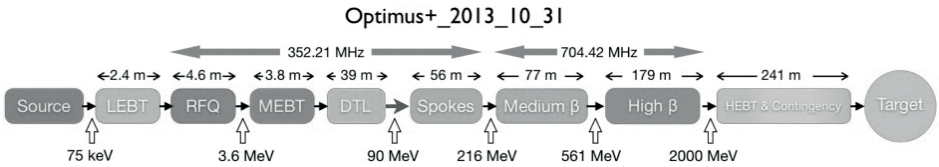

Figure 2.1: Block digram of the ESS accelerator. All segments are normal conducting except for the ”Spokes”, ”Medium β” and ”High β” segments which are superconducting.

2.3 Example of RF turn on procedure

A general transient beam loading method for phase and amplitude calibration procedure, a so called drift beam method, used at the Spallation Neutron Source (SNS) is listed below [2]:

1. Measure beam current and beam pulse shape using the beam current monitors.
2. Tune the cavity to resonance frequency.
3. Turn on RF input pulse to cavity. Turn on beam with specified beam current and pulse length.
4. Measure the phase and amplitude of the beam-induced signal.
5. Measure the phase and amplitude of the noise signal before the next beam pulse arrives. Subtract the noise signal from the beam-induced signal.
6. Repeat the measurement in step (4) for approximately ten beam pulses and average the results.
7. Predict the beam-induced signal in the model by measured beam current and beam pulse shape.
8. Determine the phase onset and amplitude calibration coefficient by comparing measured result with model calculations.
9. Set amplitude and phase.

Chapter 3
Theory

The theory for the cavity model is adapted from [3] and corroborated by [4]. The model is visualized in figure 3.1.

3.1 Cavity model - LCR circuit

Resonant LCR circuits can be used to model the resonant modes in cavities [3] [4]. As a particle passes through a RF cavity, the accelerating electric field $E(z,t)$, on the cavity axis changes due to the time varying RF field. The maximum accelerating voltage that acts on a particle, taking the transit time effect into account, is called the cavity voltage, V_{cav}. It is implied in the definition of V_{cav} that the particle passes the center of the cavity just as the accelerating voltage reaches its maximum, so called on-crest acceleration.

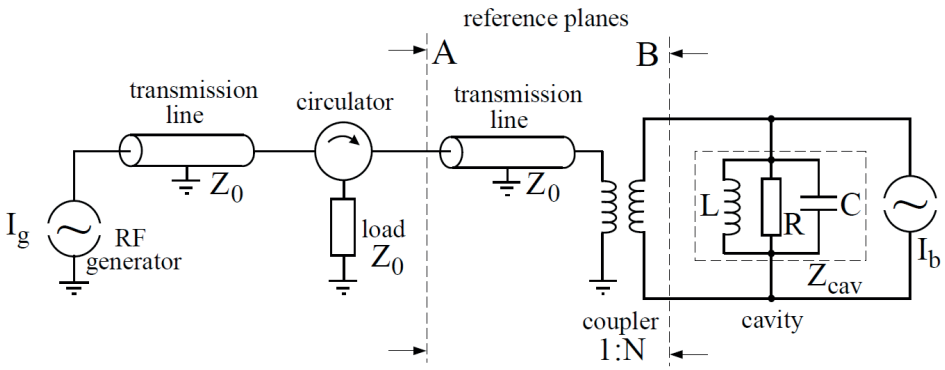

Figure 3.1: Simple circuit model of a cavity connected to a RF generator through a coupler and transmission lines. The circulator ensures that the transmission line from the RF generator is always properly terminated with forward traveling waves only. [3]

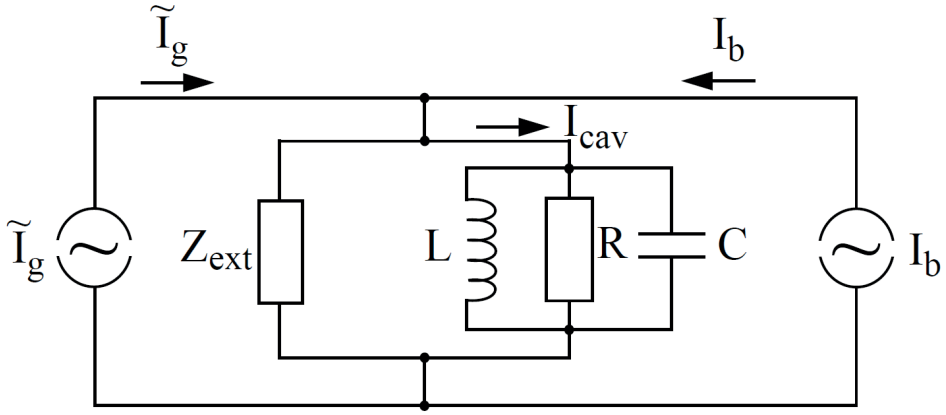

Figure 3.2: The cavity circuit model in figure 3.1 as seen from the right side of reference plane B. The external load Z_{ext} is Z_0 transformed to the cavity side of the coupler through the relation $Z_{ext} = N^2 Z_0$. [3]

It can be shown [3] that the accelerating voltage for a particle bunch passing the cavity with a time delay of t_b is

$$V_{acc}(t_b) = |\boldsymbol{V}_{cav}| \cos(\phi_b) = |\boldsymbol{V}_{cav}| \cos(\omega t_b) \tag{3.1}$$

where $V_{acc}(t_b)$ is the accelerating voltage acting on the the particles, ϕ_b is the beam phase and ω is the RF angular frequency.

To feed RF power to a cavity an input coupler is required. Providing an input coupler for each individual cavity would be prohibitively expensive, so in practice several cavities are coupled either magnetically or electrically to a coupled-resonator structure with a single RF feed point. The ”cavity segments” of such a coupled-resonator structure are usually called ”cells”, while the coupled-resonator structure itself is called ”cavity”. The ESS design at the time of writing [5] is using six electrically coupled cells in the ”Medium β” section and five electrically coupled cells in the ”High β” section, see figure 2.1.

3.2 Cavity equations and definitions

The cavity is a resonant device, and its quality factor Q is defined as

$$Q = 2\pi \frac{\text{stored energy in cavity}}{\text{energy loss per cycle}} = \frac{\omega_0 W}{P} \tag{3.2}$$

where W is the stored energy, ω_0 is the resonance angular frequency and P is the power lost per cycle.

The cavity RF field induces surface currents in the cavity walls. The surface resistance of the cavity walls together with these currents cause power dissipation. The resistor in the LCR circuit model of the cavity accounts for the power

dissipated from these surface currents. The resistor resistance R_C (called "circuit resistance" from here on) is defined as dissipating the same amount of power as the induced surface currents dissipate in the cavity, P_{diss},

$$R_C \equiv \frac{V_{cav}^2}{2P_{diss}} \Leftrightarrow P_{diss} = \frac{V_{cav}^2}{2R_C}. \tag{3.3}$$

It is useful to introduce the unloaded quality factor Q_0, which is defined as the quality factor when losses from RF surface resistance (but no other losses) are taken into account

$$Q_0 \equiv 2\pi \frac{\text{stored energy in cavity}}{\text{energy dissipated per cycle}} = \frac{\omega_0 W}{P_{diss}}. \tag{3.4}$$

The normalized shunt impedance $\left(\frac{r}{Q}\right)$ is determined by the geometry of the cavity and is independent of the surface resistance. The relation between the circuit resistance R_C and the normalized shunt impedance can be expressed as

$$R_C = \frac{1}{2}\left(\frac{r}{Q}\right) Q_0. \tag{3.5}$$

Using the LCR circuit model the stored power W and the dissipated power P_{diss} can be expressed as

$$W = \frac{CV_0^2}{2}, \qquad P_{diss} = \frac{V_0^2}{2R_C}$$

allowing the unloaded quality factor to be expressed as

$$Q_0 = \frac{\omega_0 W}{P_{diss}} = \omega_0 \frac{\frac{1}{2}CV_0^2}{\frac{V_0^2}{2R_C}} = \omega_0 R_C C \tag{3.6}$$

where V_0 is the amplitude of the oscillating voltage and C is the circuit capacitance.

In addition to the energy dissipated in the cavity walls there is energy that is extracted through the power coupler, see figure 3.1, and dissipated in an external load. The external quality factor Q_{ext} is defined as

$$2\pi \frac{\text{stored energy in cavity}}{\text{dissipated energy in external devices per cycle}} = \frac{\omega_0 W}{P_{ext}} = Q_{ext} \tag{3.7}$$

where P_{ext} is the dissipated power in all external devices. Accounting for both energy dissipation in the cavity walls and external devices is the loaded quality factor Q_L which is defined as

$$Q_L = 2\pi \frac{\text{stored energy in cavity}}{\text{total energy loss per cycle}} = \frac{\omega_0 W}{P_{tot}}. \tag{3.8}$$

Because of energy conservation

$$P_{tot} = P_{diss} + P_{ext} \tag{3.9}$$

and using equations (3.4),(3.7) and (3.8) yields

$$\frac{1}{Q_L} = \frac{1}{Q_0} + \frac{1}{Q_{ext}}. \tag{3.10}$$

The transformed external load Z_{ext}, see figure 3.2, acts as a parallel resistor to the cavity resistor R_C. They can both be replaced by a single resistor R_L, the loaded shunt impedance, with the relation

$$\frac{1}{R_L} = \frac{1}{R_C} + \frac{1}{Z_{ext}}. \tag{3.11}$$

The coupling between the cavity and the transmission line is described by the coupling factor β, which is defined as [3] [6]

$$\beta = \frac{R_C}{Z_{ext}} = \frac{R_C}{N^2 Z_0}, \qquad N = \sqrt{\frac{R_C}{\beta Z_0}} \tag{3.12}$$

where N is the transformation factor. Using this definition we can express equation 3.11 as

$$R_L = \frac{R_C}{1+\beta} \tag{3.13}$$

which together with equation (3.5) yields

$$Q_L = \frac{Q_0}{1+\beta}. \tag{3.14}$$

The coupling factor β is useful to describe the behavior of normal conducting cavities where β is in the order of one. For superconducting cavities where $Q_0 \gg Q_L$ the coupling factor is in the order of 10^3 to 10^4 and $Q_L \approx Q_{ext}$.

Another useful property is the cavity time constant τ, which is the inverse of the cavity angular bandwidth $\omega_{1/2}$ and is given by

$$\tau = \frac{1}{\omega_{1/2}} = \frac{2Q_L}{\omega_0} = \frac{Q_L}{\pi f_0} \tag{3.15}$$

where ω_0 and f_0 is the resonance frequency of the cavity expressed in radians and Hertz respectively.

3.3 Dissipated and Reflected Power of a Cavity

According to chapters 3.3.1-3.3.2 in [3] the forward and reflected power of the cavity without beam loading can be expressed as

$$P_{ref} = \left(1 - \frac{4\beta}{(\beta+1)^2}\frac{1}{1+\tan^2(\psi)}\right) P_{for} \tag{3.16}$$

where β is the coupling factor and ψ is the tuning angle of the cavity.

With beam loading the general formula for the reflected power in the cavity is

$$\begin{aligned} P_{ref} &= \frac{1}{(\beta+1)^2}\frac{1}{1+\tan^2(\psi)}\cdot \\ &\cdot \left| \left((\beta-1) + i(\beta+1)\tan(\psi)\right)\sqrt{P_g}e^{-i\Theta} + \sqrt{\frac{\beta R_C}{2}}\boldsymbol{I}_b \right|^2 \end{aligned} \tag{3.17}$$

where Θ is the angle between the positive direction of the real axis and the generator current $\boldsymbol{I}_g$, P_g is the generator power, $\boldsymbol{I}_b$ is the beam current and R_C is the circuit resistance. In terms of amplitudes Θ can be expressed through the relation

$$\cos(\Theta) = \frac{I_g^2 + I_{b0}^2 - \frac{V_{acc}^2}{(2R_L cos(\psi)\cos(\phi_b))^2}}{2I_g I_{b0}} \tag{3.18}$$

where ϕ_b is the beam phase, R_L is the load impedance, V_{acc} is the accelerating voltage and I_{b0} is the DC beam current.

In the case of a superconducting cavity expressing voltages, currents and powers in terms of β is not very useful, since β will be roughly 3 to 4 orders of magnitude greater than 1. A $\beta \gg 1$ also implies that the unloaded quality factor is much larger than the external quality factor, $Q_0 \gg Q_{ext}$, so nearly all properties depend only on the loaded quality factor Q_L. This allows for expressing the cavity properties in terms of the circuit resistance R_C and the normalized shunt impedance $\left(\frac{r}{Q}\right)$ through the approximations

$$\frac{R_C}{\beta} \approx \frac{R_C}{\beta+1} = \frac{1}{2}\left(\frac{r}{Q}\right)Q_L; \qquad \frac{\beta}{\beta+1} \approx 1 \tag{3.19}$$

which in turn leads to an approximate expression for the reflected power in a superconducting cavity

$$P_{ref} = \frac{1}{1+\tan^2(\psi)}\left|(1 + i\tan(\psi))\sqrt{P_g}e^{-i\Theta} + \frac{1}{2}\sqrt{\left(\frac{r}{Q}\right)Q_L}\boldsymbol{I}_b\right|^2. \tag{3.20}$$

The generator power P_g needed for a given field in the normal conducting case is [3]

$$\frac{V_{cav}^2}{R_L}\frac{\beta+1}{8\beta}\left(\left[1+\frac{2R_L I_{b0}}{V_{cav}}\cos(\phi_b)\right]^2+\left[\tan(\psi)+\frac{2R_L I_{b0}}{V_{cav}}\sin(\phi_b)\right]^2\right). \tag{3.21}$$

In the case of superconducting cavities the approximations in (3.19) apply so P_g is simplified to

$$\frac{V_{cav}^2}{\left(\frac{r}{Q}\right)Q_L}\frac{1}{4}\left(\left[1+\frac{\left(\frac{r}{Q}\right)Q_L I_{b0}}{V_{cav}}\cos(\phi_b)\right]^2+\left[\frac{\Delta f}{f_{1/2}}+\frac{\left(\frac{r}{Q}\right)Q_L I_{b0}}{V_{cav}}\sin(\phi_b)\right]^2\right) \tag{3.22}$$

where $f_{1/2}$ is the bandwidth of the cavity and Δf is the difference between the resonance frequency f_0 and the frequency f, i.e., $\Delta f = f_0 - f$. The differences Δf and $\Delta\omega$ are also called the *detuning*, expressed in Hertz and radians respectively.

The Lorentz forces induced by the cavity field and the beam also causes some detuning of the cavity. The Lorentz force detuning constant K is defined as [3]

$$K \equiv \frac{f_{0_1} - f_{0_2}}{E_{acc}^2} \tag{3.23}$$

where E_{acc} is the accelerating field, f_{0_1} is the initial resonance frequency, $f_0(E_{acc} = 0)$, and f_{0_2} is the final resonance frequency for when E_{acc} has reached steady state. The dynamic detuning of the cavity can be described by the first order differential equation [7]

$$\tau_m \Delta\dot{\omega}(t) + \Delta\omega(t) = -2\pi K E_{acc}^2(t) \tag{3.24}$$

where τ_m is the mechanical time constant and $\Delta\omega(t) = \omega_0(t) - \omega_{feed}$. Lorentz force detuning causes extra power consumption in the generator according to the ratio [7]

$$\rho = \left(\frac{\Delta\omega_L(t)}{\omega_{1/2}}\frac{1}{1+Q_L/Q_{L,opt}(\beta)}\right)^2 \tag{3.25}$$

where ρ is the ratio, $\omega_{1/2}$ is the angular bandwidth of the cavity, Q_L is the loaded quality factor and $Q_{L,opt}$ is the optimized loaded quality factor. This detuning can be compensated using a feed-forward error correction method, see section 3.6.1 on page 13.

3.4 Optimized cavity parameters

Part of the cavity input power can be lost at the input. The size of the losses is dependent on the coupling factor and whether the beam is present in the cavity or not. To reduce power consumption and heat generation it is important to minimize these losses.

One part of minimizing power consumption (for RF field control) in the cavity is minimizing the reflected power, preferably eliminating it completely. Part of this optimization is choosing the tuning angle such that the second bracket of equation (3.21) disappears,

$$\tan(\psi_{opt}) = -\frac{2R_L I_{b0}}{V_{cav}} \sin(\phi_b) = -\frac{2}{\beta+1} \frac{R_C I_{b0}}{V_{cav}} \sin(\phi_b) \tag{3.26}$$

where ψ_{opt} is the optimized tuning angle. The generator power with optimized tuning, $P_{g,opt}$, which is acquired by inserting (3.26) into equation (3.21) becomes

$$P_{g,opt} = \frac{V_{cav}^2}{R_L} \frac{\beta+1}{8\beta} \left[1 + \frac{2R_L I_{b0}}{V_{cav}} \cos(\phi_b)\right]. \tag{3.27}$$

The expression for the optimized coupling, β_{opt}, is obtained by differentiating $P_{g,opt}$ with respect to β, resulting in

$$\beta_{opt} = 1 + \frac{2R_C I_{b0}}{V_{cav}} \cos(\phi_b) \tag{3.28}$$

which when inserted into equation (3.27) nets an expression for the minimum generator power required to maintain a cavity voltage of V_{cav}, $P_{g,min}$,

$$P_{g,min} = \beta_{opt} \frac{V_{cav}^2}{2R_C}. \tag{3.29}$$

Using the above expression in equation (3.26) results in

$$\tan(\psi_{opt}) = -\frac{\beta_{opt}-1}{\beta_{opt}+1} \tan(\phi_b). \tag{3.30}$$

The injection time, t_{inj}, is not a cavity parameter as such, but is useful for certain methods of minimizing the power consumption of the cavity. It is calculated as

$$t_{inj} = \tau ln\left(1 + \frac{V_{cav}}{2R_L I_{b0} \cos(\phi_b)}\right) \tag{3.31}$$

where τ is the cavity time constant, V_{cav} is the cavity voltage, R_L is the loaded shunt impedance, I_{b0} is the DC current of the beam and ϕ_b is the beam phase.

3.4.1 Superconducting cavities

Applying the approximations in (3.19) to equation (3.30) shows that for superconducting cavities

$$\tan(\psi_{opt}) = -\frac{\beta_{opt}-1}{\beta_{opt}+1} \tan(\phi_b) \approx -\tan(\phi_b) \Leftrightarrow \psi_{opt} = -\phi_b \tag{3.32}$$

i.e., that the tuning angle and beam phase are equal. For the optimized coupling factor the approximations imply that

$$\beta_{opt} \approx \beta_{opt} - 1 = \frac{2R_C I_{b0}}{V_{cav}} \cos(\phi_b) \tag{3.33}$$

which when inserted into equation (3.29) yields the minimized generator power for the superconducting cavity

$$P_{g,min} = \frac{V_{cav}^2}{\left(\frac{r}{Q}\right) Q_{L,opt}} = V_{cav} I_{b0} \cos(\phi_b) \tag{3.34}$$

where $Q_{L,opt}$ is the optimized loaded quality factor. Reshuffling equation (3.34) nets the expression

$$Q_{L,opt} = \frac{V_{cav}}{\left(\frac{r}{Q}\right) I_{b0} \cos(\phi_b)} \tag{3.35}$$

which combined with equation (3.32) allows the expression of the tuning angle as

$$\tan(\psi_{opt}) = -\frac{\left(\frac{r}{Q}\right) Q_L I_{b0}}{V_{cav}} \sin(\phi_b). \tag{3.36}$$

If the difference between the generator angle frequency ω and the cavity resonance frequency ω_0 is sufficiently small, which is the case here, the tuning angle can be approximated as

$$\tan(\psi) \approx 2Q_L \frac{\Delta\omega}{\omega} = 2Q_L \frac{\Delta f}{f} \tag{3.37}$$

where Δw and Δf is the detuning expressed in radians and Hertz respectively. In the case of an optimized tuning angle this leads to

$$\tan(\psi_{opt}) = 2Q_L \frac{\Delta\omega_{opt}}{\omega} = -\frac{\left(\frac{r}{Q}\right) Q_L I_{b0}}{V_{cav}} \sin(\phi_b)$$

implying that

$$\frac{\Delta\omega_{opt}}{\omega} = -\frac{\left(\frac{r}{Q}\right) I_{b0}}{2V_{cav}} \sin(\phi_b). \tag{3.38}$$

3.5 Optimization of cavity filling - pre-detuning

Cavity filling refers to the charging of the cavity to obtain the desired cavity field. This is done by feeding the cavity with RF power. If the cavity is detuned the cavity voltage will oscillate with the detuning frequency during the filling, requiring more RF power to obtain the same cavity field voltage during the same filling period [8].

In order to minimize power consumption the detuning has to be compensated for. This is done by modulating the phase of the RF power feed to track the cavity resonance frequency [8]. The phase is modulated according to

$$\Delta\phi(t) = \int_0^1 \Delta\omega(\tau) d\tau \tag{3.39}$$

where $\Delta\phi(t)$ is the phase modulation and $\Delta\omega(\tau)$ is the measured detuning during the cavity filling. Since the phase modulation is based on the measured detuning, using frequency tracking requires that the detuning is accurately measured and transmitted to the RF power feed without significant delay.

3.6 Error correction control

In the cavity model the beam is treated as a perturbation to the otherwise stable cavity field. The purpose of error correction control is to compensate for that perturbation so the cavity field maintains the planned voltage and provides the beam particles the correct acceleration.

3.6.1 Feed-forward

A feed-forward error correction method aims to predict the beam and its errors from simulations and past data from similar scenarios and preemptively make adjustments for any errors. The beam, the cavity and their interactions must be predictable over time in order for error correction based on old or simulated data to work. It is also crucial to match the correction with the incoming beam, otherwise both the correction and the beam will cause perturbation to the field, see figure 3.3.

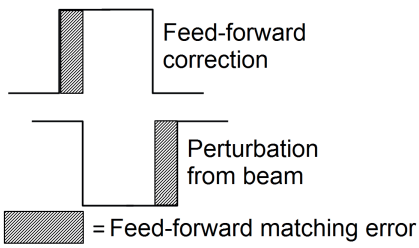

Figure 3.3: Schematic figure of feed-forward matching error.

3.6.2 Feed-back

A feed-back error correction method corrects for errors using some formula based on data measured in real time. A common implementation of feed-back error correction is the PID regulator where the signal adjustment is based on the sign of the current error, the size of the error over time and whether the size of the error is increasing or decreasing at the moment.

One issue with feed-back error correction is that it has a limited frequency response. There is some delay, however short, from measuring the error to implementing changes to the cavity. Because of the very short timescales in the acceleration process this delay may cause the cavity to adjust to a situation that has already passed by the time the adjustments are made, creating an error instead of compensating for one.

3.7 Beam position monitoring

In order to determine a viable combination of beam current and pulse length the impact on the beam position monitoring, BPM, system must be taken into account. The BPM system measures the phase and position of the proton beam. The phase measurements are required to tune downstream cavities and the position measurements are necessary to steer the beam and ensure that it does not deviate from its projected path.

The ESS linear accelerator will include more than 140 beam position monitors (BPMs) of various types and sizes. The BPMs will primarily measure the beam position and phase, but will also provide a rough estimate of beam intensity. One requirement of the ESS BPM system is that it must be able to measure the beam's position and phase even when it is significantly de-bunched [9]. The signal-to-noise ratio (S/N) of the BPM signals degrades as the beam is de-bunched, resulting in less accurate measurements. It is still crucial to measure the beam position to ensure that the beam does not deviate from the projected path and damages the equipment.

Several parameters, including beam velocity, button size and beam pipe diameter, affect the amplitude of the signal induced in a BPM button [9]. Since these parameters vary along the linear accelerator electronics will be used to level-adjust, down-convert, filter and condition the BPM signals before sending them on to a digitizer module. The signals are then sampled and fed to a field programmable gate array, FPGA, for digital signal processing to determine the beam position, phase and intensity [9].

The ESS linear accelerator will have pipe segments that are 60 mm and 100 mm in diameter. The smaller pipes will be used for the lower energy sections of the accelerator such as the MEBT, DTL and Spoke cavities in figure 2.1 in section 2.2. The larger pipes are for the higher energy sections of the accelerator such as the medium β and high β in figure 2.1 in section 2.2. The RF feed frequency will be 352.21 MHz in the smaller pipe sections and 704.42 MHz in the larger pipe sections.

The design at the time of writing requires the BPMs to measure the beam position with an accuracy (rms) of 100 µm and a resolution of 20 µm [9]. The beam phase measurement must have an accuracy (rms) of 1° and a resolution of 0.2° [9].

3.7.1 Button BPM

Button BPMs are a cost-efficient and compact implementation of a BPM that uses a circular insulated metal plate for detection. The plate diameter can vary, from several mm to several cm [10]. The BPMs are usually installed in a circular arrangement around the beam pipe, with two BPMs each for the X and Y directions, see figure 3.4.

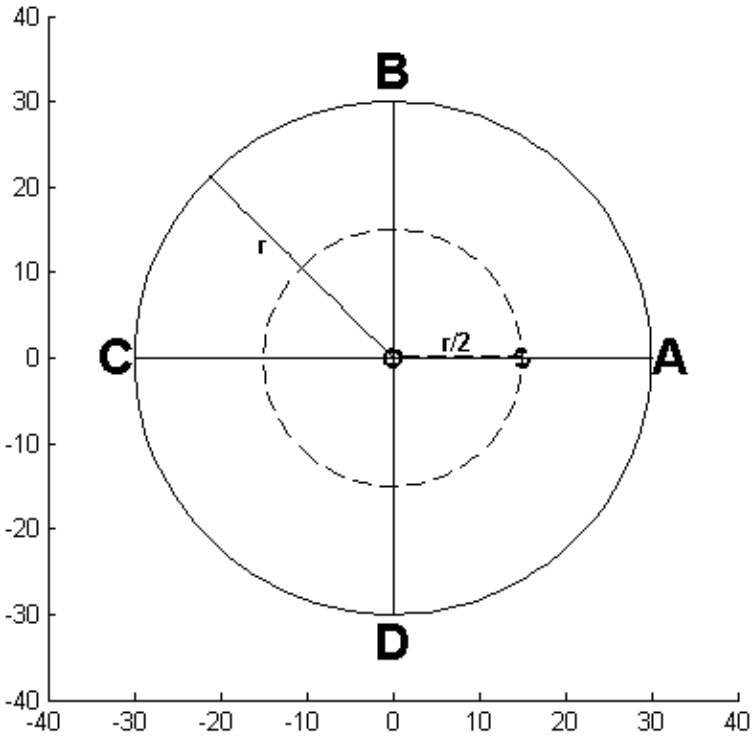

Figure 3.4: Pipe beam crossection with button BPM positioning. The letters indicate the BPMs.

3.8 Expected BPM resolution for position measurement

The expected BPM resolution for four distinct scenarios is shown in table 3.1, along with the scenario parameters. The position resolution has been calculated for a centered beam from the S/N ratio. The noise figure used for the calculations is composed of the sum of the effective input noise from the front-end electronics and the thermal noise for an analog bandwidth of 10 MHz at room temperature [11]. The resolution of the phase measurements is expected to be almost completely unaffected by the effective input noise and the thermal noise. Instead the dominant source of error will be the jitter of the ADC clock. The rough estimation of the phase error in table 3.1 is based on an assumption of 1 ps of clock jitter [11]. For scenarios A and B the phase measurement is assumed to be made from direct sampling at 352 MHz, while for scenarios C and D it is assumed to be made from sampling at an intermediate frequency, this explains the difference in expected accuracy.

Table 3.1: Scenario parameters and corresponding calculated resolutions [11]

Case	Beam pipe diameter, ∅	Proton energy, E	Coupling factor, β	Button BPM position resolution	Stripline BPM position resolution	Rough estimate of phase resolution
A	60 mm	92 MeV	0.41	3.32 µm	2.53 µm	0.13°
B	60 mm	217 MeV	0.58	4.69 µm	2.64 µm	0.13°
C	100 mm	217 MeV	0.58	6.20 µm	2.29 µm	0.02°
D	100 mm	2 GeV	0.95	10.16 µm	2.67 µm	0.02°

To conduct time of flight (TOF) measurements, the beam phase at two BPM locations is compared to each other. The phase difference is proportional to the beam velocity, so the TOF measurements can be used to calculate the beam energy. A larger distance between the measurement points gives smaller measurement errors for the phase measurement, but also limits the phase measurement range. Larger distances between the BPMs used may also add to technical complexity [11]. For higher particle energies, and thus higher particle speeds, the size of the relative error in the online energy measurements increases.

3.8.1 Non-optimal conditions

When the conditions for BPM measurements are non-optimal, such as when the beam has a short pulse width, a low current or is de-bunched, the accuracy decreases. Large errors will occur if the pulse width is shorter than the electronics settling time, which as of early 2014 was expected to be about 1-2 µs [11]. When no cavities are powered beyond the spokes session, such as during beam commissioning, the longitudinal beam size will increase by approximately 100 mm for every 150 m it travels. Thus when the beam reaches the junction between the accelerator and target it will have a bunch length of approximately 330 mm. This will cause a large overlap between successive bunches and decrease the amplitude of the 352 MHz harmonic by three orders of magnitude, making the BPM resolution extremely poor. If this is combined with a lower beam current it will drown the 352 MHz harmonic in noise.

3.9 Analytic modeling of button BPM signal strength

The theory behind the analytic modeling in this section can be found in [12] and [13]. The proton beam induces a current in the button BPM called the image current, I_{img}. The image current can be expressed as

$$I_{img}(\omega) = \frac{\pi r_{button}^2}{2\pi} \frac{i\omega r_{pipe}}{\beta c} 2I_{beam}(\omega) \tag{3.40}$$

where r_{button} is the button radius, r_{pipe} is the pipe radius, β is the fraction of light speed the protons are moving at, c is the speed of light, I_{beam} is the beam current and ω is the RF feed frequency in radians. The button impedance Z can be expressed as

$$Z(\omega) = \frac{Z_0}{Z_0 i\omega C_{button} + 1} \tag{3.41}$$

where Z_0 is the characteristic impedance and C_{button} is the parasitic capacitance of the button BPM. The voltage induced in the button BPM, V_{button} is given by

$$V_{button}(\omega) = Z(\omega) I_{img}(\omega) = \frac{\pi r_{button}^2 i\omega}{2\pi r_{pipe} \beta c} \frac{Z_0}{Z_0 i\omega C_{button} + 1} I_{beam}(\omega). \tag{3.42}$$

Signal strength in regards to BPMs is more commonly expressed in dBm which is obtained using

$$S_{button} = 10 log_{10}(\frac{V_{button}^2}{2Z_0}) \tag{3.43}$$

where S_{button} is the signal strength of the button BPM in dBm.

Chapter 4

Cavity simulations

The purpose of the cavity simulations was two-fold:

- To determine combinations of feed pulse length and feed pulse current that do not cause larger perturbations to the cavity accelerating field than permitted by the ESS requirements.
- To find an energy-efficient RF input pulse shape for loading the cavity.

The simulations focused on the normal conducting cavities, the MEBT and the DTL in figure 2.1, but some simulations of the superconducting cavities were made for comparison.

4.1 The Model

The simulink model used for the simulations is created by Rihua Zeng based on the theoretical model described in section 3.1. The top layer of the model is shown in figure 4.1. The corresponding graphical user interface is shown in figure 4.7 on page 23.

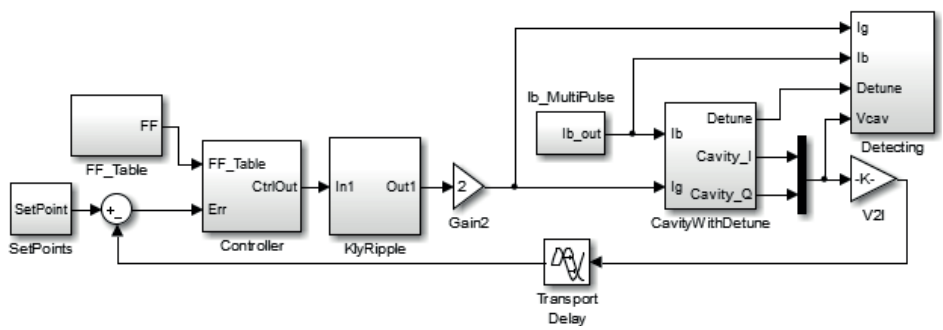

Figure 4.1: Simulink model for cavity filling simulations. The grey rectangles, referred to as boxes in the text, indicate subroutines.

The SetPoints subroutine generates the RF input pulse shape taking into account the transport delay and eventual phase shifting from the feedforward error control. The FF_Table subroutine contains the feed-forward error correction signal that is sent to the controller subroutine. If feed-back error correction is enabled it is applied in the ”Controller” subroutine. If feed-back error correction is disabled the input from the ”FF_Table” subroutine passes unaltered to the ”KlyRipple” subroutine. Perturbations from rippling in the klystron is added to the phase and amplitude of the incoming signal in the ”KlyRipple” subroutine, see figure 4.2. The amplitude perturbations are assumed to be negligible and set to zero. The beam current is generated in the ”Ib_MultiPulse” subroutine, see figure 4.3 for details. The cavity simulations are performed in the ”CavityWithDetune” subroutine which uses the beam and generator currents as inputs and provides the current, quality factor and detuning as outputs. Simulation data is collected in the ”Detecting” subroutine and converted to the desired output units.

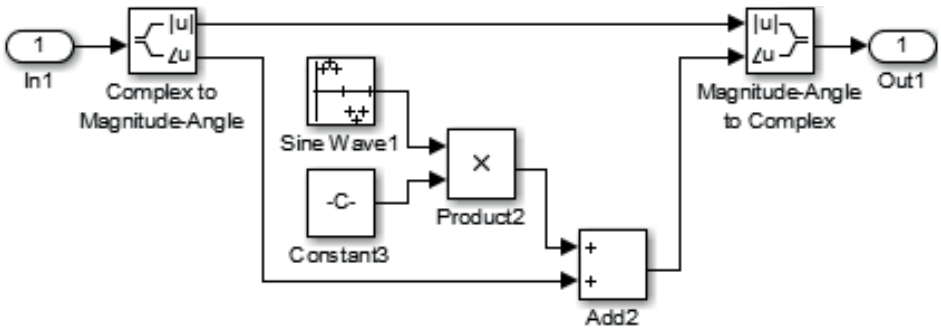

Figure 4.2: Detail of Simulink model, KlyRipple subroutine. The signal amplitude is unaltered since ”Sine Wave1” has an amplitude of zero.

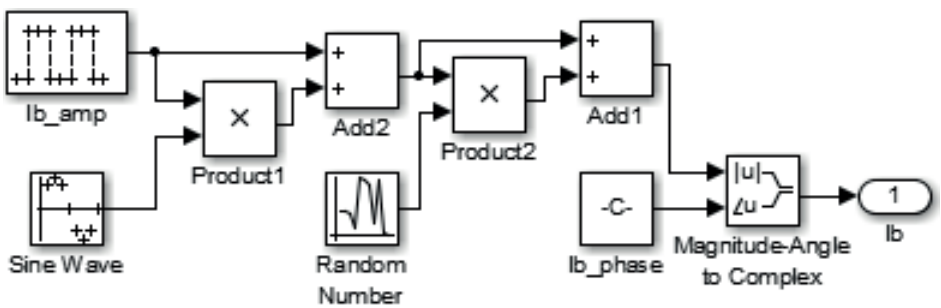

Figure 4.3: Detail of Simulink model, ”Ib_Multipulse” subroutine. A sine wave perturbation and a random number perturbation are added to the beam current amplitude to simulate the variance of the beam current.

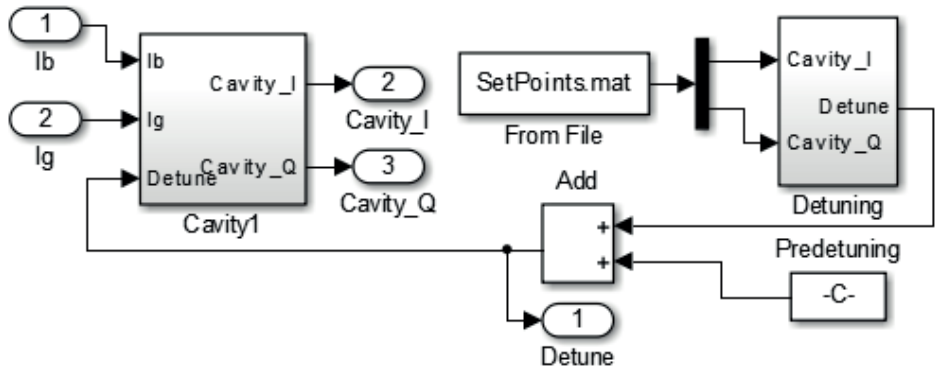

Figure 4.4: Detail of Simulink model, "CavityWithDetune" subroutine. Detuning is calculated as the sum of the detuning from cavity filling, calculated using the RF input pulse, and the predetuning. Ideally this detuning is close to zero.

The subroutine for generating the feed-forward error correction signal is shown in figure 4.6 on page 23. The subroutine calculates a new generator current I_g that compensates for the beam current and the cavity detuning. The real part of the new generator current, I_{gr}, is simply the previous generator current appended with the measured beam current. The imaginary part of the new generator current, I_{gi}, is calculated based on the difference between the measured detuning and the calculated pre-detuning. Note that while the model does simulate the variance of the beam current between pulses *it does not account for inexactness in measuring the beam current*. The beam current generated in the "Ib_MultiPulse" subroutine is used both for cavity perturbation simulation and for generating the feed-forward error correction signal.

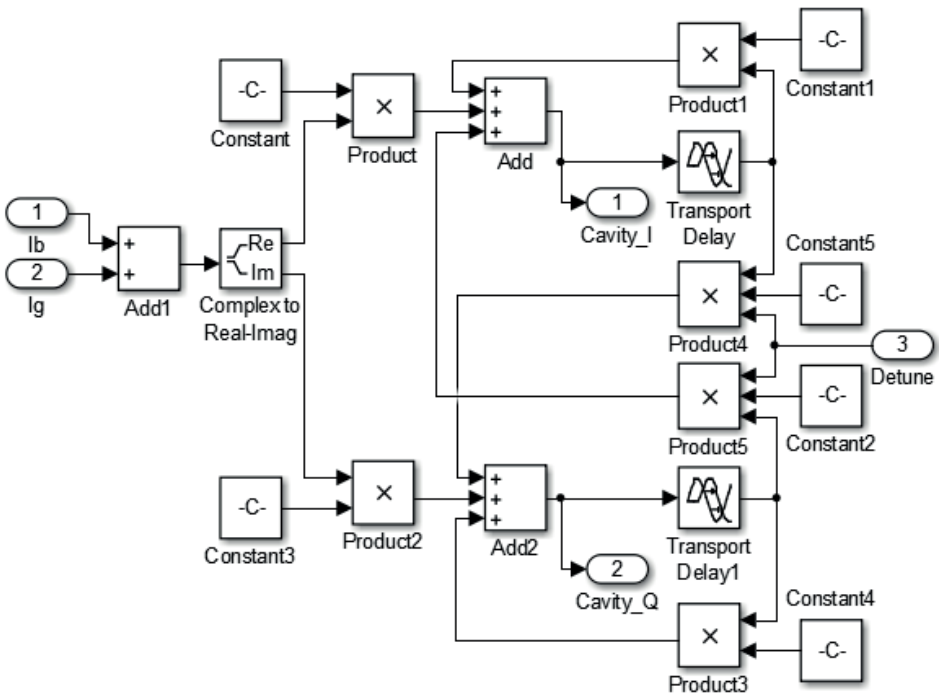

Figure 4.5: Detail of Simulink model, ”Cavity1” subroutine. This subroutine implements the cavity theory in chapter 3 and is used to calculate the current and quality factor of the cavity.

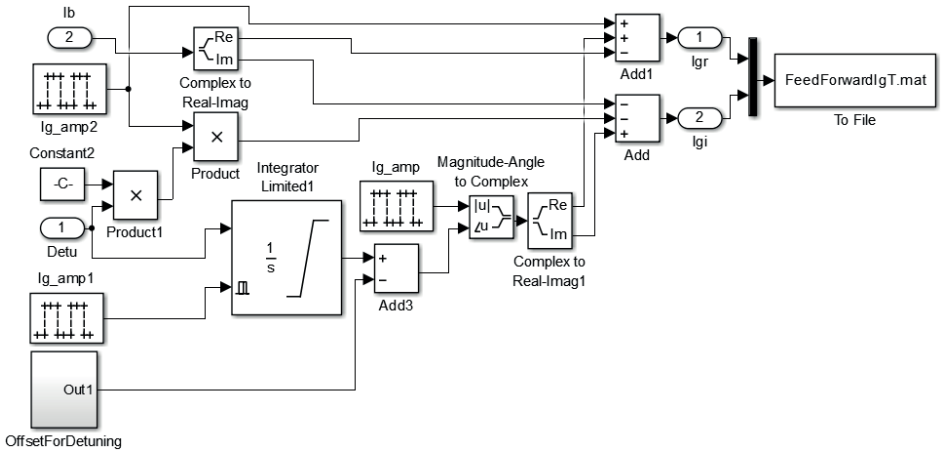

Figure 4.6: Detail of Simulink model, ”Detecting\FFTableWrite” subroutine. This subroutine generates the signal used for feed-forward error correction using the beam current and detuning as inputs. Note that the same beam current is used for both cavity simulation and feed-forward error correction signal generation, implying perfect measurement of beam current and phase.

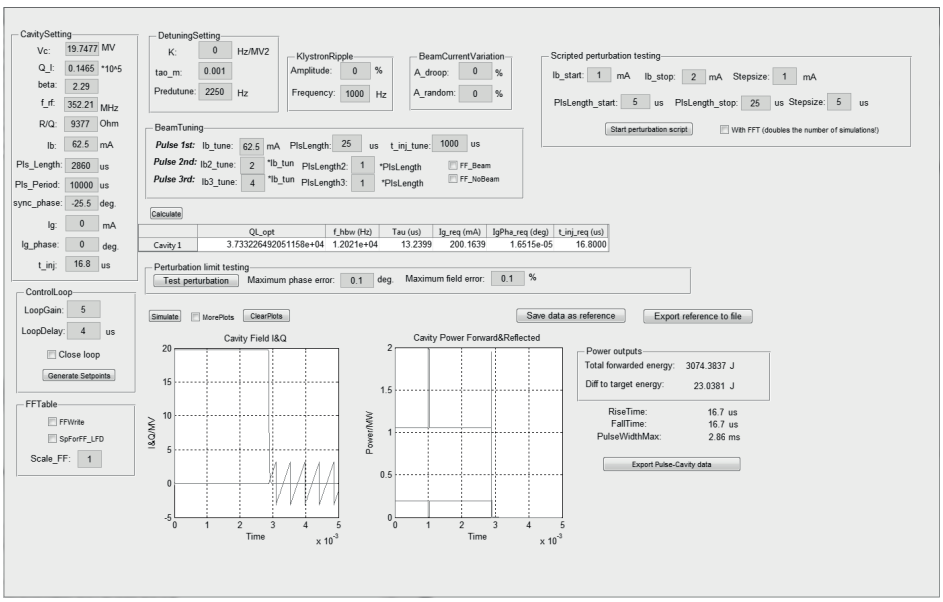

Figure 4.7: Graphical user interface for simulink model.

4.2 Calculating optimized input values

4.2.1 Normal conducting cavity simulations

For the purpose of the simulations a number of parameters were given. The beam power P_{beam} and the beam current I_{b0} are the desired outputs that the design aims to produce. Simulations tailored to the desired beam parameters then provide the dissipated power P_{diss}, the unloaded quality factor Q_0 and the beam phase $\phi_{b,d}$. The feed frequency f_{feed} and the cavity time constant τ are design parameters related to the cavity. The pulse length T_B is another output parameter constricted by design considerations further down the accelerator line. All the given parameter values are shown in table 4.1.

Table 4.1: Given parameter values for the normal conducting cavity

Parameter	Value	Unit
P_{beam}	1.114	MW
I_{b0}	62.5	mA
P_{diss}	1.078	MW
Q_0	44455	[1]
$\phi_{b,d}$	-25.5	degrees
f_{feed}	352.21	MHz
τ	13.24	µs
T_B	2860	µs

To allow for some margin of error the dissipated power P_{diss} is 25 % larger than the minimum value given by simulations. This "safe" P_{diss} value is included in the given Q_0 value.

Assuming ideal matching the reflected power will be zero in the steady state and the optimized coupling factor, β_{opt}, can be obtained through

$$\beta_{opt} = 1 + \frac{P_{beam}}{P_{diss}} \tag{4.1}$$

where P_{beam} is the beam power and P_{diss} is the dissipated power. With β_{opt} known the loaded quality factor Q_L is calculated using equation (3.14)

$$Q_L = \frac{Q_0}{1 + \beta_{opt}}$$

which together with equation (3.15) gives the resonance frequency of the cavity, f_0, and subsequently the detuning frequency Δf

$$f_0 = \frac{Q_L}{\pi\tau} = f_{feed} + \Delta f \Leftrightarrow \Delta f = \frac{Q_L}{\pi\tau} - f_{feed}$$

where τ is the cavity time constant and f_{feed} is the feed frequency.

The necessary generator power P_g is given by

$$P_g = P_{diss} + P_{beam} \tag{4.2}$$

which implicitly includes the error margin from P_{diss}. The tuning angle is calculated from equation (3.30),

$$\tan(\psi) = -\frac{\beta - 1}{\beta + 1}\tan(\phi_b)$$

where ϕ_b is $\phi_{b,d}$ in radians. The cavity voltage is derived from the beam parameters

$$V_{cav} = \frac{P_{beam}}{I_{b0}\cos(\phi_b)} \tag{4.3}$$

and is used to calculate the circuit resistance, see equation (3.3),

$$R_C = \frac{V_{cav}^2}{2P_{diss}}.$$

With R_C known, the load resistance R_L is calculated using equation (3.13),

$$R_L = \frac{R_C}{\beta_{opt} + 1}$$

which allows for the normalized shunt impedance $\left(\frac{r}{Q}\right)$ to be calculated using equations (3.5),(3.13) and (3.14),

$$\left(\frac{r}{Q}\right) = \frac{2R_L}{Q_L}.$$

The results of the calculations in this section are found in table 4.2.

Table 4.2: Initial input values for the normal conducting cavity

Property	Value	Unit
V_{cav}	19.7477	MW
Q_l	14650	[1]
β_0	2.29	[1]
f_{rf}	352.21	MHz
r/Q	9377	Ω
I_{b0}	62.5	mA
T_B	2860	µs
$\phi_{b,d}$	-25.5	degrees
t_{inj}	16.8	µs
Δf	2250	Hz

4.2.2 Superconducting cavity simulations

For the purpose of the simulations a number of parameters were given. The beam current I_{b0} is the desired output. The cavity voltage V_{cav}, the normalized shunt impedance $\left(\frac{r}{Q}\right)$ and the beam phase $\phi_{b,d}$ are determined by simulations tailored to reach the desired beam current, these simulations are however outside of the scope of this report. The feed frequency f_{feed} is an input value determined by previous stages of the accelerator and the pulse length T_B is determined by later stages of the accelerator. All the given parameter values are shown in table 4.3.

Table 4.3: Given parameter values for the superconducting cavity

Parameter	Value	Unit
V_{cav}	21.3	MV
f_{feed}	352.21	MHz
$\left(\frac{r}{Q}\right)$	7106	Ω
I_{b0}	50	mA
$\phi_{b,d}$	-24	degrees
T_B	2860	µs

The loaded quality factor Q_L is calculated using equation (3.35) as

$$Q_L = \frac{V_{cav}}{\left(\frac{r}{Q}\right) I_{b0} \cos(\phi_b)}$$

where ϕ_b is $\phi_{b,d}$ expressed in radians. This allows for the loaded shunt impedance R_L to be calculated using equation (3.13) as

$$R_L = \frac{\left(\frac{r}{Q}\right) Q_L}{2}.$$

Using equations (3.32) and (3.37) the detuning Δf is obtained from

$$\Delta f = \frac{\tan(\phi_b) f_{feed}}{2Q_L}$$

where ϕ_b is $\phi_{b,d}$ expressed in radians. The resonance angular frequency ω_0 of the cavity is given by

$$\omega_0 = 2\pi(\Delta f + f_{feed}) \tag{4.4}$$

and can be used to determine the cavity time constant τ from equation (3.15),

$$\tau = \frac{2Q_L}{\omega_0}$$

which allows the calculation of the injection time t_{inj} using equation (3.31),

$$t_{inj} = \tau ln\left(1 + \frac{V_{cav}}{2R_L I_{b0} \cos(\phi_b)}\right).$$

The results of the calculations in this section are found in table 4.4.

Table 4.4: Initial input values for the superconducting cavity

Parameter	Value	Unit
V_{cav}	21.3	MV
Q_L	131245	[1]
f_{feed}	352.21	MHz
$\left(\frac{r}{Q}\right)$	7106	Ω
I_{b0}	50	mA
T_B	2860	µs
$\phi_{b,d}$	-24	degrees
t_{inj}	48.1	µs
Δf	1195	Hz

4.3 Cavity filling - Cavity response for different RF input pulse shapes

Each input pulse generates a corresponding cavity response, a curve with a certain *rise time*. All pulses eventually reach the current required to produce the desired cavity voltage steady-state, I_{req}, but differ in shape before that point, see figure 4.8a. Six different input pulses were used in the simulations. The evaluated input pulses consisted of three different linear slope inputs, with rise times of 3, 6 and 12 τ, an exponential slope input with a rise time of 6 τ, a single-step pulse and a two-step pulse. The resulting cavity response curves are shown in figure 4.8b and the corresponding rise times are shown in table 4.5.

The simplest pulse is a single step of constant input of I_{req}, resulting in a moderate rise time and causing some notable power reflection. The two-step pulse adds a short initial step where $I > I_{req}$ before abruptly transitioning to the second step where $I = I_{req}$. This shortens the rise time significantly but also causes significant power reflection in the initial stage, see figure 4.9. This power reflection is likely to trigger the interlock and shut the beam down in order to protect the klystron.

A way to avoid power reflection is to ramp up the current over time from a low initial level, this naturally results in a longer rise time. Results vary depending on the shape and the inclination of the slope. Notably all the sloped pulses produce less reflected power during the rise than during the steady-state, suggesting that rise times longer than 3 τ are unnecessary. A potential draw-back of this ramp-up approach is that the klystron will be dumping the excess current, converting it to heat. Depending on the klystron this heat could be a problem, but the ESS klystron will have sufficient capacity to handle it [14]. Even so the power savings in the cavity might not translate to power savings in the ESS facility as a whole.

Table 4.5: Cavity filling rise times

Pulse type	Rise time [µs]
Two-step	36
Single-step	79.7
$6 - \tau$ exponential	109.5
$3 - \tau$ linear	105.2
$6 - \tau$ linear	138
$12 - \tau$ linear	210.3

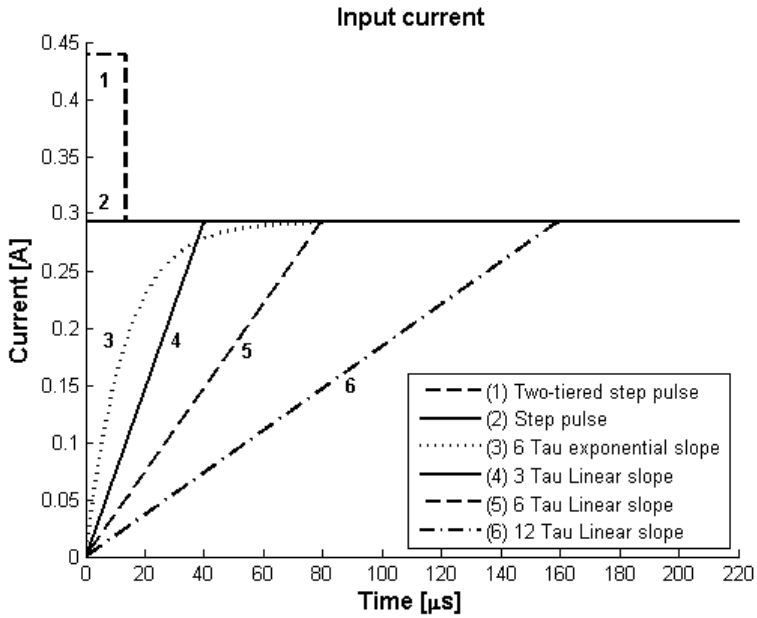

(a) RF input pulse shapes.

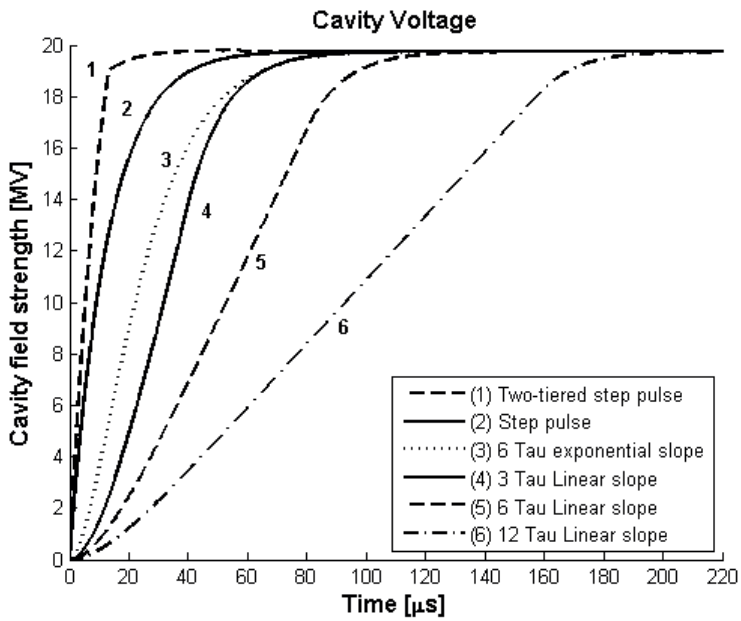

(b) Cavity responses for different RF input pulse shapes.

Figure 4.8: RF input pulse shapes and the corresponding cavity responses.

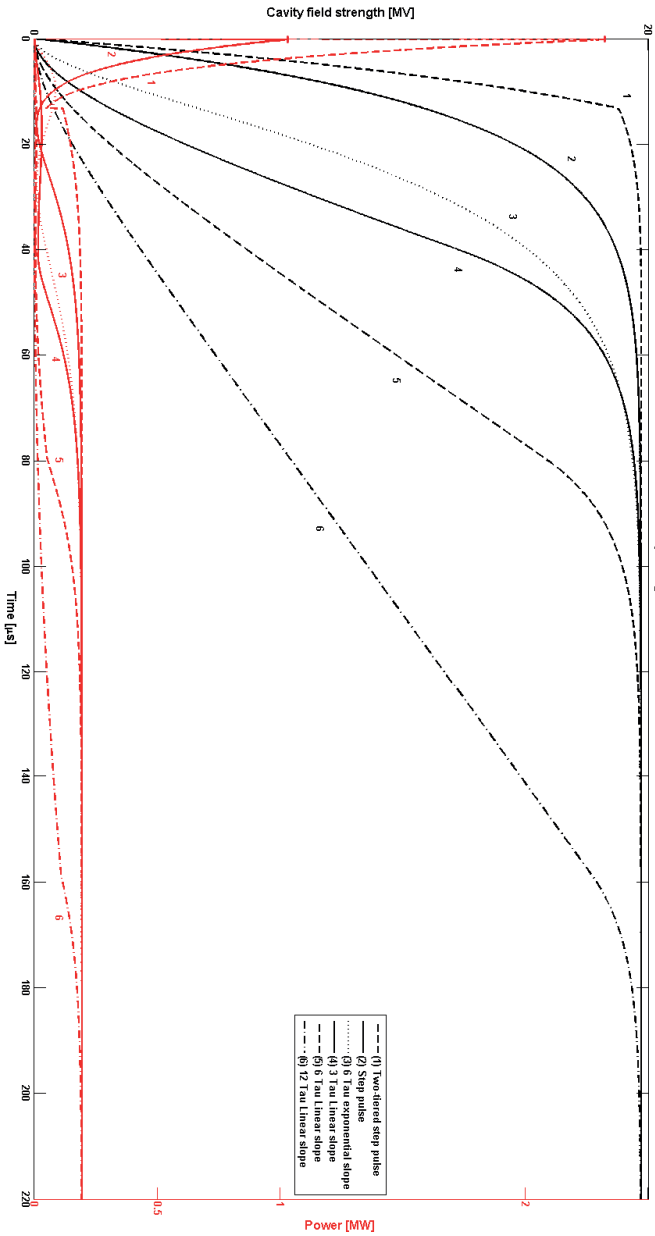

Figure 4.9: Reflected power for different cavity filling curves.

4.4 Cavity perturbation from beam loading

The purpose of the simulations was to find cavity and beam settings that would provide a stable cavity field strength in order to properly accelerate the beam. This information would then be used to find the most cost-efficient design of the accelerator.

When the beam arrives at the cavity it causes a perturbation to the otherwise stable cavity field, see figure 4.10. The size of the perturbation depends on the beam current and the beam pulse length as well as the error correction system and its settings. If the perturbation is large it will significantly alter the acceleration of the beam, mismatching it with sections down the line and potentially damaging them.

Part of the purpose of the simulations was to find combinations of beam current and beam pulse length that would not cause perturbations to the cavity field larger than the given error limits for each cavity field control system. The parameters of interest was the cavity field strength and phase. The initial error limits were 1 % of cavity field strength and 1° of phase. Stricter limits of 0.5 % of cavity field strength and 0.5° of phase were later introduced, followed by the even stricter limits of 0.1 % of cavity field strength and 0.1° of phase that are in use at the time of writing.

Some initial simulations were conducted to roughly determine viable beam pulse lengths and currents for phase scan simulations. From these results it was decided to test beam currents from 2.5 mA to 62.5 mA in steps of 2 mA for beam pulse lengths of 1 µs to 20 µs in steps of 1 µs.

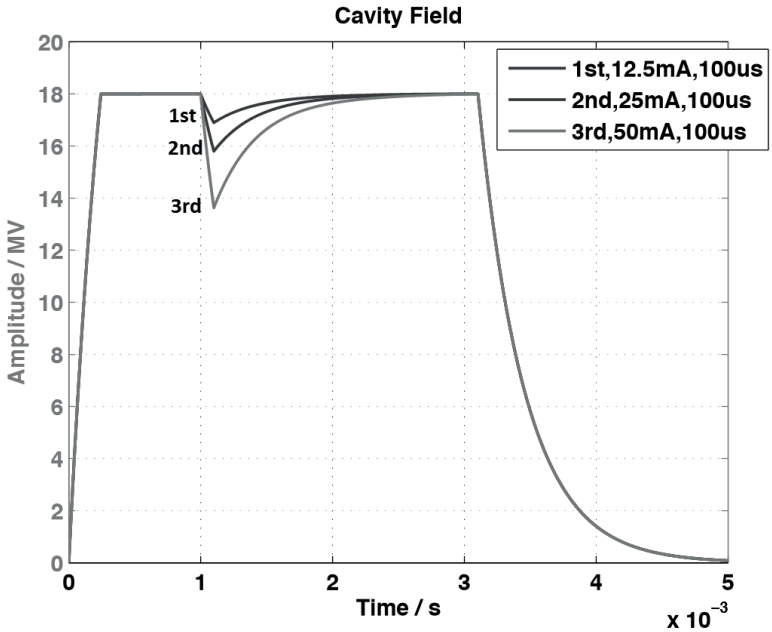

(a) Cavity response to perturbations from beams with different currents but equal pulse lengths.

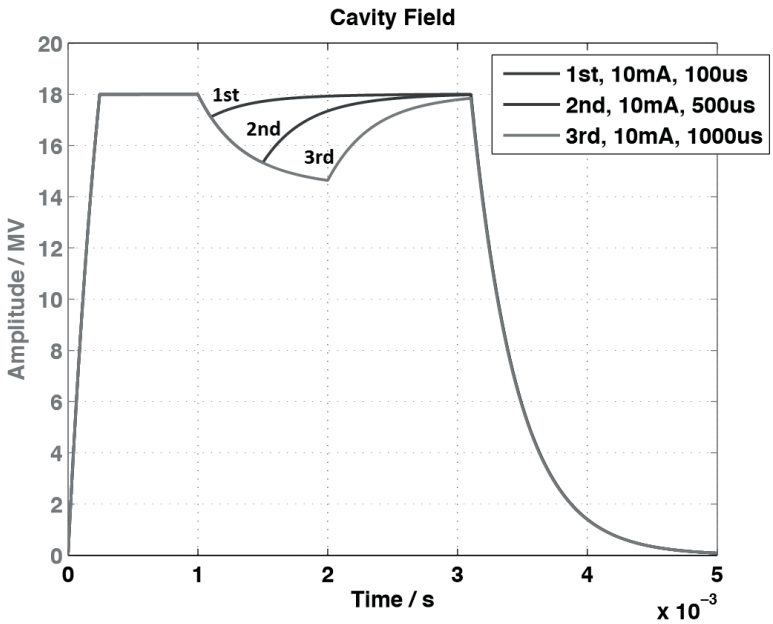

(b) Cavity response to perturbations from beams with equal currents but different pulse lengths.

Figure 4.10: Typical cavity response to the perturbation from a proton beam.

4.4.1 Normal conducting cavity

Simulations were conducted using the input values in table 4.2 with the exception of the beam current, which was adjusted from 2.5 mA to 62.5 mA in steps of 2 mA. The beam pulse length was adjusted from 1 µs to 20 µs in steps of 1 µs. These beam pulse lengths are suitable for phase scanning, normal operation will be using a pulse length of 2.86 ms. Simulations were conducted for the following cavity settings:

- Using no feed-forward or feed-back error correction.
- Using feed-back error correction with a loop gain of 2.
- Using feed-back error correction with a loop gain of 5.
- Using feed-forward error correction with a matching error of 0.1 µs.
- Using feed-forward error correction with a matching error of 1 µs.
- Using feed-forward and feed-back error correction. The feed-forward having a matching error of 1 µs and the feed-back having a loop gain of 2.
- Using feed-forward and feed-back error correction. The feed-forward having a matching error of 1 µs and the feed-back having a loop gain of 5.

The feed-forward error correction matching error was implemented as a static delay to the feed-forward table. The magnitude of the mismatch depends on how precisely the cavity tuning can be adjusted. A mismatch of 1 µs corresponds to a detuning of 100 MHz, while a mismatch of 0.1 µs corresponds to a detuning of 10 MHz. Precise tuning on this scale is complicated, but possible to achieve. For the feed-back error correction the loop gain of 5 is the highest reasonable value to implement in practice.

The simulation data was saved and tested in a separate script against the three increasingly stricter error limits. The results were collected in spreadsheets showing which combinations of beam current and beam pulse length passed both tests, failed the field strength test, failed the phase test or failed both tests, for the three different sets of error limits. The spreadsheets also included information about the size of the maximum errors for failed combinations, both for field strength and phase.

The error limits were only checked for the maximum error, so the results do not differentiate between a spike error or a continuous error. Neither do the results differentiate between positive and negative deviations from the desired values, only the magnitude of the errors was investigated. This is in accordance with the requested tolerance levels however, continuous errors within the error limits are considered manageable while spike errors outside the limits are not.

4.4.2 Superconducting cavity

Simulations were conducted using the input values in table 4.2 with the exception of the beam current, which was adjusted from 2.5 mA to 62.5 mA in steps of 2 mA. The beam pulse length was adjusted from 1 µs to 20 µs in steps of 1 µs. Simulations were conducted for the following cavity settings:

- Using no feed-forward or feed-back error correction and a Lorentz force detuning constant of zero.
- Using no feed-forward or feed-back error correction and a Lorentz force detuning constant of 30.

The simulation data was saved and tested in a separate script against the three increasingly stricter error limits. The results were collected in spreadsheets in the same manner as the normal conducting cavity results.

Again, the error limits were only checked for the maximum error, so the results do not differentiate between a spike error or a continuous error. Neither do the results differentiate between positive and negative deviations from the desired values, only the magnitude of the errors was investigated.

4.5 Cavity perturbation simulation results

4.5.1 Using no feed-forward or feed-back error correction

With no error correction the size of the perturbation depends only on the beam current and beam pulse length. Figure 4.11 shows the results of the simulations. The error limit pertaining to the cavity field strength proved to be the harder limit to keep as can be seen from the numbers of twos in figure 4.11.

Technically it would be possible to use neither feed-forward nor feed-back error correction as long as the beam current is kept low and the pulse length short. In practice this would put high demands on the beam chopper to produce the short pulse length as well as significantly increase the wear and tear the beam chopper is subjected to. High wear and tear means equipment has to be replaced often, causing facility downtime and extra expenses.

Perturbation limit tests of field voltage and phase for 1 % and 1 degree error limits:
Key: 0 = Passes both tests, 1 = Fails both tests, 2 = Fails field test, 3 = Fails phase test

Beam current	Pulse length in us:																			
in mA:	1	2	3	4	5	6	7	8	9	10	11	12	13	14	15	16	17	18	19	20
2.5	0	0	0	0	0	0	0	0	0	0	0	0	0	0	2	2	2	2	2	2
4.5	0	0	0	0	0	2	2	2	2	2	2	2	2	2	2	2	2	2	2	2
6.5	0	0	0	2	2	2	2	2	2	2	2	2	2	2	2	2	2	1	1	1
8.5	0	0	2	2	2	2	2	2	2	2	2	1	1	1	1	1	1	1	1	1
10.5	0	0	2	2	2	2	2	2	1	1	1	1	1	1	1	1	1	1	1	1
12.5	0	2	2	2	2	2	2	1	1	1	1	1	1	1	1	1	1	1	1	1
14.5	0	2	2	2	2	1	1	1	1	1	1	1	1	1	1	1	1	1	1	1
16.5	0	2	2	2	2	1	1	1	1	1	1	1	1	1	1	1	1	1	1	1
18.5	0	2	2	2	1	1	1	1	1	1	1	1	1	1	1	1	1	1	1	1
20.5	0	2	2	1	1	1	1	1	1	1	1	1	1	1	1	1	1	1	1	1
22.5	2	2	2	1	1	1	1	1	1	1	1	1	1	1	1	1	1	1	1	1

Perturbation limit tests of field voltage and phase for 0.5 % and 0.5 degree error limits:
Key: 0 = Passes both tests, 1 = Fails both tests, 2 = Fails field test, 3 = Fails phase test

Beam current	Pulse length in us:																			
in mA:	1	2	3	4	5	6	7	8	9	10	11	12	13	14	15	16	17	18	19	20
2.5	0	0	0	0	0	2	2	2	2	2	2	2	2	2	2	2	2	2	2	2
4.5	0	0	2	2	2	2	2	2	2	2	1	1	1	1	1	1	1	1	1	1
6.5	0	2	2	2	2	1	1	1	1	1	1	1	1	1	1	1	1	1	1	1
8.5	0	2	2	2	2	1	1	1	1	1	1	1	1	1	1	1	1	1	1	1
10.5	0	2	2	1	1	1	1	1	1	1	1	1	1	1	1	1	1	1	1	1
12.5	2	2	2	1	1	1	1	1	1	1	1	1	1	1	1	1	1	1	1	1

Perturbation limit tests of field voltage and phase for 0.1 % and 0.1 degree error limits:
Key: 0 = Passes both tests, 1 = Fails both tests, 2 = Fails field test, 3 = Fails phase test

Beam current	Pulse length in us:																			
in mA:	1	2	3	4	5	6	7	8	9	10	11	12	13	14	15	16	17	18	19	20
2.5	2	2	2	1	1	1	1	1	1	1	1	1	1	1	1	1	1	1	1	1
4.5	2	1	1	1	1	1	1	1	1	1	1	1	1	1	1	1	1	1	1	1
6.5	2	1	1	1	1	1	1	1	1	1	1	1	1	1	1	1	1	1	1	1

Figure 4.11: The results of the cavity perturbation simulation using no feed-forward or feed-back error correction.

4.5.2 Using feed-back error correction

Applying feed-back error correction to the cavity is a clear improvement, see figure 4.12. Using a loop gain of 5 provided slightly better results than using a loop gain of 2.

The results are not great however, the maximum current is limited 10.5 mA and that is only possible with a pulse length of just 1 µs.

Perturbation limit tests of field voltage and phase for 1 % and 1 degree error limits:
Key: 0 = Passes both tests, 1 = Fails both tests, 2 = Fails field test, 3 = Fails phase test

Beam current	Pulse length in us:																		
in mA:	1	2	3	4	5	6	7	8	9	10	11	12	13	14	15	16	17	18	19	20
2.5	0	0	0	0	0	0	0	0	0	0	0	0	0	0	0	0	0	0	0	0
4.5	0	0	0	0	0	0	0	0	0	0	0	0	0	0	0	0	0	0	0	0
6.5	0	0	0	0	0	0	0	0	0	0	0	0	0	0	0	0	0	0	0	0
8.5	0	0	0	0	0	0	0	0	0	0	0	0	0	0	0	0	0	0	0	0
10.5	0	0	2	2	2	2	2	2	2	2	2	2	2	2	2	2	2	2	2	2
12.5	0	2	2	2	2	2	2	2	2	2	2	2	2	2	2	2	2	2	2	2
14.5	0	2	2	2	2	2	2	2	2	2	2	2	2	2	2	2	2	2	2	2
16.5	0	2	2	2	2	2	2	2	2	2	2	2	2	2	2	2	2	2	2	2
18.5	0	2	2	2	2	2	2	2	2	2	2	2	2	2	2	2	2	2	2	2
20.5	0	2	2	2	2	2	2	2	2	2	2	2	2	2	2	2	2	2	2	2

Perturbation limit tests of field voltage and phase for 0.5 % and 0.5 degree error limits:
Key: 0 = Passes both tests, 1 = Fails both tests, 2 = Fails field test, 3 = Fails phase test

Beam current	Pulse length in us:																		
in mA:	1	2	3	4	5	6	7	8	9	10	11	12	13	14	15	16	17	18	19	20
2.5	0	0	0	0	0	0	0	0	0	0	0	0	0	0	0	0	0	0	0	0
4.5	0	0	0	0	0	0	0	0	0	0	0	0	0	0	0	0	0	0	0	0
6.5	0	2	2	2	2	2	2	2	2	2	2	2	2	2	2	2	2	2	2	2
8.5	0	2	2	2	2	2	2	2	2	2	2	2	2	2	2	2	2	2	2	2
10.5	0	2	2	2	2	2	2	2	2	2	2	2	2	2	2	2	2	2	2	2

Perturbation limit tests of field voltage and phase for 0.1 % and 0.1 degree error limits:
Key: 0 = Passes both tests, 1 = Fails both tests, 2 = Fails field test, 3 = Fails phase test

Beam current	Pulse length in us:																		
in mA:	1	2	3	4	5	6	7	8	9	10	11	12	13	14	15	16	17	18	19	20
2.5	1	1	1	1	1	1	1	1	1	1	1	1	1	1	1	1	1	1	1	1

Figure 4.12: The results of the cavity perturbation simulation using feed-back error correction with a loop gain of 5.

4.5.3 Using feed-forward error correction

With feed-forward error correction and a matching error of 1 µs the results are significantly improved over both the case of no feed-forward/feed-back error correction and using feed-back error correction, see figure 4.13. The cavity field error also appears to be independent of the beam pulse length, giving the same error magnitude for all tested pulse lengths. This is because the feed-forward error correction signal is calculated assuming perfect measurement of the beam current and phase, providing a near-perfect correction signal. Thus the dominating error source is the feed-forward matching error which is independent of pulse length.

Using Feed-Forward table and a FFT matching error of 1us
Perturbation limit tests of field voltage and phase for 1 % and 1 degree error limits:
Key: 0 = Passes both tests, 1 = Fails both tests, 2 = Fails field test, 3 = Fails phase test

Beam current in mA:	Pulse length in us: 1	2	3	4	5	6	7	8	9	10	11	12	13	14	15	16	17	18	19	20
2.5	0	0	0	0	0	0	0	0	0	0	0	0	0	0	0	0	0	0	0	0
4.5	0	0	0	0	0	0	0	0	0	0	0	0	0	0	0	0	0	0	0	0
6.5	0	0	0	0	0	0	0	0	0	0	0	0	0	0	0	0	0	0	0	0
8.5	0	0	0	0	0	0	0	0	0	0	0	0	0	0	0	0	0	0	0	0
10.5	0	0	0	0	0	0	0	0	0	0	0	0	0	0	0	0	0	0	0	0
12.5	0	0	0	0	0	0	0	0	0	0	0	0	0	0	0	0	0	0	0	0
14.5	0	0	0	0	0	0	0	0	0	0	0	0	0	0	0	0	0	0	0	0
16.5	0	0	0	0	0	0	0	0	0	0	0	0	0	0	0	0	0	0	0	0
18.5	0	0	0	0	0	0	0	0	0	0	0	0	0	0	0	0	0	0	0	0
20.5	0	0	0	0	0	0	0	0	0	0	0	0	0	0	0	0	0	0	0	0
22.5	2	2	2	2	2	2	2	2	2	2	2	2	2	2	2	2	2	2	2	2

Using Feed-Forward table and a FFT matching error of 1us
Perturbation limit tests of field voltage and phase for 0.5 % and 0.5 degree error limits:
Key: 0 = Passes both tests, 1 = Fails both tests, 2 = Fails field test, 3 = Fails phase test

Beam current in mA:	Pulse length in us: 1	2	3	4	5	6	7	8	9	10	11	12	13	14	15	16	17	18	19	20
2.5	0	0	0	0	0	0	0	0	0	0	0	0	0	0	0	0	0	0	0	0
4.5	0	0	0	0	0	0	0	0	0	0	0	0	0	0	0	0	0	0	0	0
6.5	0	0	0	0	0	0	0	0	0	0	0	0	0	0	0	0	0	0	0	0
8.5	0	0	0	0	0	0	0	0	0	0	0	0	0	0	0	0	0	0	0	0
10.5	0	0	0	0	0	0	0	0	0	0	0	0	0	0	0	0	0	0	0	0
12.5	2	2	2	2	2	2	2	2	2	2	2	2	2	2	2	2	2	2	2	2

Using Feed-Forward table and a FFT matching error of 1us
Perturbation limit tests of field voltage and phase for 0.1 % and 0.1 degree error limits:
Key: 0 = Passes both tests, 1 = Fails both tests, 2 = Fails field test, 3 = Fails phase test

Beam current in mA:	Pulse length in us: 1	2	3	4	5	6	7	8	9	10	11	12	13	14	15	16	17	18	19	20
2.5	2	2	2	2	2	2	2	2	2	2	2	2	2	2	2	2	2	2	2	2
4.5	2	2	2	2	2	2	2	2	2	2	2	2	2	2	2	2	2	2	2	2
6.5	2	2	2	2	2	2	2	2	2	2	2	2	2	2	2	2	2	2	2	2
8.5	1	1	1	1	1	1	1	1	1	1	1	1	1	1	1	1	1	1	1	1

Figure 4.13: The results of the cavity perturbation simulation using feed-forward error correction and a matching error of 1 µs.

Simulations with feed-forward error correction and a matching error of just 0.1 µs show that both the cavity field strength and the cavity phase stay within the error limits for all tested beam currents and beam pulse lengths at the medium error limits of 0.5 % field strength and 0.5° phase. Under the strict limits of 0.1 % field strength and 0.1° phase all tested pulse lengths stay within the error limits for beam currents up to 20.5 mA.

4.5.4 Using feed-forward and feed-back error correction

Simulations using both feed-forward and feed-back error correction showed disappointing results. While the results are superior to using only feed-back error correction they are worse than using feed-forward correction alone, see figure 4.14 for a comparison. Interestingly a loop gain of 5 produces worse results than a loop gain of 2, despite the better results of the higher loop gain in the pure feed-back simulations.

Using Feed-Forward table and a FFT matching error of 1us
Perturbation limit tests of field voltage and phase for 0.5 % and 0.5 degree error limits:
Key: 0 = Passes both tests, 1 = Fails both tests, 2 = Fails field test, 3 = Fails phase test

Beam current in mA:	Pulse length in us:																			
	1	2	3	4	5	6	7	8	9	10	11	12	13	14	15	16	17	18	19	20
2.5	0	0	0	0	0	0	0	0	0	0	0	0	0	0	0	0	0	0	0	0
4.5	0	0	0	0	0	0	0	0	0	0	0	0	0	0	0	0	0	0	0	0
6.5	0	0	0	0	0	0	0	0	0	0	0	0	0	0	0	0	0	0	0	0
8.5	0	0	0	0	0	0	0	0	0	0	0	0	0	0	0	0	0	0	0	0
10.5	0	0	0	0	0	0	0	0	0	0	0	0	0	0	0	0	0	0	0	0
12.5	2	2	2	2	2	2	2	2	2	2	2	2	2	2	2	2	2	2	2	2

Using Feed-Forward and feed-back, FFT matching error of 1us, loop gain of 5
Perturbation limit tests of field voltage and phase for 0.5 % and 0.5 degree error limits:
Key: 0 = Passes both tests, 1 = Fails both tests, 2 = Fails field test, 3 = Fails phase test

Beam current in mA:	Pulse length in us:																			
	1	2	3	4	5	6	7	8	9	10	11	12	13	14	15	16	17	18	19	20
2.5	0	0	0	0	0	0	0	0	0	0	0	0	0	0	0	0	0	0	0	0
4.5	0	0	0	0	0	0	0	0	0	0	0	0	0	0	0	0	0	0	0	0
6.5	0	0	2	2	2	0	0	0	0	0	0	0	0	0	0	0	0	0	0	0
8.5	0	2	2	2	2	2	0	0	0	2	2	2	2	0	0	0	0	2	2	2
10.5	0	2	2	2	2	2	0	0	0	2	2	2	2	2	0	0	0	2	2	2
12.5	2	2	2	2	2	2	2	2	2	2	2	2	2	2	2	2	2	2	2	2

Using Feed-Forward and feed-back, FFT matching error of 1us, loop gain of 2
Perturbation limit tests of field voltage and phase for 0.5 % and 0.5 degree error limits:
Key: 0 = Passes both tests, 1 = Fails both tests, 2 = Fails field test, 3 = Fails phase test

Beam current in mA:	Pulse length in us:																			
	1	2	3	4	5	6	7	8	9	10	11	12	13	14	15	16	17	18	19	20
2.5	0	0	0	0	0	0	0	0	0	0	0	0	0	0	0	0	0	0	0	0
4.5	0	0	0	0	0	0	0	0	0	0	0	0	0	0	0	0	0	0	0	0
6.5	0	0	0	0	0	0	0	0	0	0	0	0	0	0	0	0	0	0	0	0
8.5	0	0	0	0	0	0	0	0	0	0	0	0	0	0	0	0	0	0	0	0
10.5	0	0	0	2	2	2	2	2	2	2	2	2	2	2	2	2	2	2	2	2

Figure 4.14: Comparison of combined feed-back and feed-forward error correction, using a feed-forward matching error of 1 µs. The top section is using no feed-back, the middle section is using feed-back with a loop gain of 2 and the bottom section is using feed-back with a loop gain of 5.

4.5.5 Superconducting cavity using no error correction

Simulations on the superconducting cavity were performed with a Lorentz force detuning constant of zero as well as 30, see figure 4.15 and figure 4.16 respectively. Compensating for the Lorentz force detuning has a small but positive effect on the results.

Perturbation limit tests of field voltage and phase for 1 % and 1 degree error limits:
Key: 0 = Passes both tests, 1 = Fails both tests, 2 = Fails field test, 3 = Fails phase test

Beam current in mA:	Pulse length in us:																			
	1	2	3	4	5	6	7	8	9	10	11	12	13	14	15	16	17	18	19	20
2.5	0	0	0	0	0	0	0	0	0	0	0	0	0	0	0	0	0	0	0	0
4.5	0	0	0	0	0	0	0	0	0	0	0	0	0	0	0	0	0	0	0	0
6.5	0	0	0	0	0	0	0	0	0	0	0	0	0	0	0	0	0	0	0	0
8.5	0	0	0	0	0	0	0	0	0	0	0	0	0	0	0	0	0	0	0	0
10.5	0	0	0	0	0	0	0	0	0	0	0	0	0	0	0	0	0	0	0	0
12.5	0	0	0	0	0	0	0	0	0	0	0	0	0	0	0	0	0	0	0	0
14.5	0	0	0	0	0	0	0	0	0	0	0	0	0	0	0	0	0	0	0	0
16.5	0	0	0	0	0	0	0	0	0	0	0	0	0	0	0	0	0	0	0	0
18.5	0	0	0	0	0	0	0	0	0	0	0	0	0	0	0	0	0	0	0	0
20.5	0	0	0	0	0	0	0	0	0	0	0	0	0	0	0	0	0	0	3	3
22.5	0	0	0	0	0	0	0	0	0	0	0	0	0	0	0	0	3	3	3	3
24.5	0	0	0	0	0	0	0	0	0	0	0	0	0	0	0	3	3	3	3	3
26.5	0	0	0	0	0	0	0	0	0	0	0	0	0	0	3	3	3	3	3	3
28.5	0	0	0	0	0	0	0	0	0	0	0	0	0	3	3	3	3	3	3	3
30.5	0	0	0	0	0	0	0	0	0	0	0	0	3	3	3	3	3	3	3	1
32.5	0	0	0	0	0	0	0	0	0	0	0	3	3	3	3	3	3	3	1	1
34.5	0	0	0	0	0	0	0	0	0	0	3	3	3	3	3	3	3	1	1	1
36.5	0	0	0	0	0	0	0	0	0	0	3	3	3	3	3	3	1	1	1	1
38.5	0	0	0	0	0	0	0	0	0	3	3	3	3	3	3	1	1	1	1	1
40.5	0	0	0	0	0	0	0	0	0	3	3	3	3	3	1	1	1	1	1	1
42.5	0	0	0	0	0	0	0	0	3	3	3	3	3	1	1	1	1	1	1	1
44.5	0	0	0	0	0	0	0	0	3	3	3	3	3	1	1	1	1	1	1	1
46.5	0	0	0	0	0	0	0	0	3	3	3	3	1	1	1	1	1	1	1	1
48.5	0	0	0	0	0	0	0	3	3	3	3	1	1	1	1	1	1	1	1	1
50.5	0	0	0	0	0	0	0	3	3	3	3	1	1	1	1	1	1	1	1	1
52.5	0	0	0	0	0	0	0	3	3	3	3	1	1	1	1	1	1	1	1	1
54.5	0	0	0	0	0	0	3	3	3	3	1	1	1	1	1	1	1	1	1	1
56.5	0	0	0	0	0	0	3	3	3	3	1	1	1	1	1	1	1	1	1	1
58.5	0	0	0	0	0	0	3	3	3	1	1	1	1	1	1	1	1	1	1	1
60.5	0	0	0	0	0	0	3	3	3	1	1	1	1	1	1	1	1	1	1	1
62.5	0	0	0	0	0	0	3	3	3	1	1	1	1	1	1	1	1	1	1	1

Perturbation limit tests of field voltage and phase for 0.5 % and 0.5 degree error limits:
Key: 0 = Passes both tests, 1 = Fails both tests, 2 = Fails field test, 3 = Fails phase test

Beam current in mA:	Pulse length in us:																			
	1	2	3	4	5	6	7	8	9	10	11	12	13	14	15	16	17	18	19	20
2.5	0	0	0	0	0	0	0	0	0	0	0	0	0	0	0	0	0	0	0	0
4.5	0	0	0	0	0	0	0	0	0	0	0	0	0	0	0	0	0	0	0	0
6.5	0	0	0	0	0	0	0	0	0	0	0	0	0	0	0	0	0	0	0	0
8.5	0	0	0	0	0	0	0	0	0	0	0	0	0	0	0	0	0	0	0	0
10.5	0	0	0	0	0	0	0	0	0	0	0	0	0	0	0	0	0	0	3	3
12.5	0	0	0	0	0	0	0	0	0	0	0	0	0	0	0	0	0	3	3	3
14.5	0	0	0	0	0	0	0	0	0	0	0	0	0	0	0	0	3	3	3	3
16.5	0	0	0	0	0	0	0	0	0	0	0	0	0	0	0	3	3	3	3	3
18.5	0	0	0	0	0	0	0	0	0	0	0	0	0	0	3	3	3	3	3	1
20.5	0	0	0	0	0	0	0	0	0	0	0	0	0	3	3	3	3	3	1	1
22.5	0	0	0	0	0	0	0	0	0	0	0	0	3	3	3	3	3	1	1	1
24.5	0	0	0	0	0	0	0	0	0	0	0	3	3	3	3	3	1	1	1	1
26.5	0	0	0	0	0	0	0	0	0	0	3	3	3	3	3	1	1	1	1	1
28.5	0	0	0	0	0	0	0	0	0	3	3	3	3	3	3	1	1	1	1	1
30.5	0	0	0	0	0	0	0	0	3	3	3	3	3	3	1	1	1	1	1	1
32.5	0	0	0	0	0	0	0	3	3	3	3	3	3	1	1	1	1	1	1	1
34.5	0	0	0	0	0	0	0	3	3	3	3	3	1	1	1	1	1	1	1	1
36.5	0	0	0	0	0	0	3	3	3	1	1	1	1	1	1	1	1	1	1	1
38.5	0	0	0	0	0	0	3	3	3	1	1	1	1	1	1	1	1	1	1	1
40.5	0	0	0	0	0	3	3	3	1	1	1	1	1	1	1	1	1	1	1	1
42.5	0	0	0	0	0	3	3	1	1	1	1	1	1	1	1	1	1	1	1	1
44.5	0	0	0	0	0	3	3	1	1	1	1	1	1	1	1	1	1	1	1	1
46.5	0	0	0	0	0	3	3	1	1	1	1	1	1	1	1	1	1	1	1	1
48.5	0	0	0	3	3	1	1	1	1	1	1	1	1	1	1	1	1	1	1	1
50.5	0	0	0	3	3	1	1	1	1	1	1	1	1	1	1	1	1	1	1	1
52.5	0	0	0	3	3	1	1	1	1	1	1	1	1	1	1	1	1	1	1	1
54.5	0	0	0	3	3	1	1	1	1	1	1	1	1	1	1	1	1	1	1	1
56.5	0	0	0	3	3	1	1	1	1	1	1	1	1	1	1	1	1	1	1	1
58.5	0	0	0	3	1	1	1	1	1	1	1	1	1	1	1	1	1	1	1	1
60.5	0	0	0	3	1	1	1	1	1	1	1	1	1	1	1	1	1	1	1	1
62.5	0	0	0	3	1	1	1	1	1	1	1	1	1	1	1	1	1	1	1	1

Perturbation limit tests of field voltage and phase for 0.1 % and 0.1 degree error limits:
Key: 0 = Passes both tests, 1 = Fails both tests, 2 = Fails field test, 3 = Fails phase test

Beam current in mA:	Pulse length in us:																			
	1	2	3	4	5	6	7	8	9	10	11	12	13	14	15	16	17	18	19	20
2.5	3	3	3	3	3	3	3	3	3	3	3	3	3	3	3	3	3	3	3	3
4.5	3	3	3	3	3	3	3	3	3	3	3	3	1	1	1	1	1	1	1	1
6.5	3	3	3	3	3	3	3	3	1	1	1	1	1	1	1	1	1	1	1	1
8.5	3	3	3	3	3	3	1	1	1	1	1	1	1	1	1	1	1	1	1	1
10.5	3	3	3	3	3	1	1	1	1	1	1	1	1	1	1	1	1	1	1	1
12.5	3	3	3	3	1	1	1	1	1	1	1	1	1	1	1	1	1	1	1	1
14.5	3	3	3	1	1	1	1	1	1	1	1	1	1	1	1	1	1	1	1	1
16.5	3	3	3	1	1	1	1	1	1	1	1	1	1	1	1	1	1	1	1	1
18.5	3	3	1	1	1	1	1	1	1	1	1	1	1	1	1	1	1	1	1	1
20.5	3	3	1	1	1	1	1	1	1	1	1	1	1	1	1	1	1	1	1	1
22.5	3	3	1	1	1	1	1	1	1	1	1	1	1	1	1	1	1	1	1	1
24.5	3	3	1	1	1	1	1	1	1	1	1	1	1	1	1	1	1	1	1	1
26.5	3	1	1	1	1	1	1	1	1	1	1	1	1	1	1	1	1	1	1	1
28.5	3	1	1	1	1	1	1	1	1	1	1	1	1	1	1	1	1	1	1	1
30.5	3	1	1	1	1	1	1	1	1	1	1	1	1	1	1	1	1	1	1	1
32.5	3	1	1	1	1	1	1	1	1	1	1	1	1	1	1	1	1	1	1	1
34.5	3	1	1	1	1	1	1	1	1	1	1	1	1	1	1	1	1	1	1	1
36.5	3	1	1	1	1	1	1	1	1	1	1	1	1	1	1	1	1	1	1	1
38.5	3	1	1	1	1	1	1	1	1	1	1	1	1	1	1	1	1	1	1	1
40.5	3	1	1	1	1	1	1	1	1	1	1	1	1	1	1	1	1	1	1	1
42.5	3	1	1	1	1	1	1	1	1	1	1	1	1	1	1	1	1	1	1	1
44.5	3	1	1	1	1	1	1	1	1	1	1	1	1	1	1	1	1	1	1	1
46.5	3	1	1	1	1	1	1	1	1	1	1	1	1	1	1	1	1	1	1	1
48.5	3	1	1	1	1	1	1	1	1	1	1	1	1	1	1	1	1	1	1	1
50.5	3	1	1	1	1	1	1	1	1	1	1	1	1	1	1	1	1	1	1	1
52.5	1	1	1	1	1	1	1	1	1	1	1	1	1	1	1	1	1	1	1	1

Figure 4.15: The results of the superconducting cavity perturbation simulation with a Lorentz force constant of zero.

Perturbation limit tests of field voltage and phase for 1 % and 1 degree error limits:
Key: 0 = Passes both tests, 1 = Fails both tests, 2 = Fails field test, 3 = Fails phase test

Beam current in mA:	Pulse length in us:																			
	1	2	3	4	5	6	7	8	9	10	11	12	13	14	15	16	17	18	19	20
2.5	0	0	0	0	0	0	0	0	0	0	0	0	0	0	0	0	0	0	0	0
4.5	0	0	0	0	0	0	0	0	0	0	0	0	0	0	0	0	0	0	0	0
6.5	0	0	0	0	0	0	0	0	0	0	0	0	0	0	0	0	0	0	0	0
8.5	0	0	0	0	0	0	0	0	0	0	0	0	0	0	0	0	0	0	0	0
10.5	0	0	0	0	0	0	0	0	0	0	0	0	0	0	0	0	0	0	0	0
12.5	0	0	0	0	0	0	0	0	0	0	0	0	0	0	0	0	0	0	0	0
14.5	0	0	0	0	0	0	0	0	0	0	0	0	0	0	0	0	0	0	0	0
16.5	0	0	0	0	0	0	0	0	0	0	0	0	0	0	0	0	0	0	0	0
18.5	0	0	0	0	0	0	0	0	0	0	0	0	0	0	0	0	0	0	0	0
20.5	0	0	0	0	0	0	0	0	0	0	0	0	0	0	0	0	0	3	3	
22.5	0	0	0	0	0	0	0	0	0	0	0	0	0	0	0	0	3	3	3	3
24.5	0	0	0	0	0	0	0	0	0	0	0	0	0	0	0	3	3	3	3	3
26.5	0	0	0	0	0	0	0	0	0	0	0	0	0	3	3	3	3	3	3	3
28.5	0	0	0	0	0	0	0	0	0	0	0	0	3	3	3	3	3	3	3	3
30.5	0	0	0	0	0	0	0	0	0	0	0	0	3	3	3	3	3	3	3	1
32.5	0	0	0	0	0	0	0	0	0	0	0	3	3	3	3	3	3	3	1	1
34.5	0	0	0	0	0	0	0	0	0	0	3	3	3	3	3	3	3	1	1	1
36.5	0	0	0	0	0	0	0	0	0	0	3	3	3	3	3	3	1	1	1	1
38.5	0	0	0	0	0	0	0	0	0	3	3	3	3	3	3	1	1	1	1	1
40.5	0	0	0	0	0	0	0	0	0	3	3	3	3	3	1	1	1	1	1	1
42.5	0	0	0	0	0	0	0	0	3	3	3	3	3	1	1	1	1	1	1	1
44.5	0	0	0	0	0	0	0	0	3	3	3	3	3	1	1	1	1	1	1	1
46.5	0	0	0	0	0	0	0	3	3	3	3	3	1	1	1	1	1	1	1	1
48.5	0	0	0	0	0	0	0	3	3	3	3	3	1	1	1	1	1	1	1	1
50.5	0	0	0	0	0	0	0	3	3	3	3	1	1	1	1	1	1	1	1	1
52.5	0	0	0	0	0	0	0	3	3	3	3	1	1	1	1	1	1	1	1	1
54.5	0	0	0	0	0	0	3	3	3	3	1	1	1	1	1	1	1	1	1	1
56.5	0	0	0	0	0	0	3	3	3	3	1	1	1	1	1	1	1	1	1	1
58.5	0	0	0	0	0	0	3	3	3	3	1	1	1	1	1	1	1	1	1	1
60.5	0	0	0	0	0	0	3	3	3	3	1	1	1	1	1	1	1	1	1	1
62.5	0	0	0	0	0	0	3	3	3	3	1	1	1	1	1	1	1	1	1	1

Perturbation limit tests of field voltage and phase for 0.5 % and 0.5 degree error limits:
Key: 0 = Passes both tests, 1 = Fails both tests, 2 = Fails field test, 3 = Fails phase test

Beam current in mA:	Pulse length in us:																			
	1	2	3	4	5	6	7	8	9	10	11	12	13	14	15	16	17	18	19	20
2.5	0	0	0	0	0	0	0	0	0	0	0	0	0	0	0	0	0	0	0	0
4.5	0	0	0	0	0	0	0	0	0	0	0	0	0	0	0	0	0	0	0	0
6.5	0	0	0	0	0	0	0	0	0	0	0	0	0	0	0	0	0	0	0	0
8.5	0	0	0	0	0	0	0	0	0	0	0	0	0	0	0	0	0	0	0	0
10.5	0	0	0	0	0	0	0	0	0	0	0	0	0	0	0	0	0	3	3	3
12.5	0	0	0	0	0	0	0	0	0	0	0	0	0	0	0	0	3	3	3	3
14.5	0	0	0	0	0	0	0	0	0	0	0	0	3	3	3	3	3	3	3	3
16.5	0	0	0	0	0	0	0	0	0	0	0	3	3	3	3	3	3	3	1	1
18.5	0	0	0	0	0	0	0	0	0	0	3	3	3	3	3	3	1	1	1	1
20.5	0	0	0	0	0	0	0	0	0	3	3	3	3	3	1	1	1	1	1	1
22.5	0	0	0	0	0	0	0	0	3	3	3	3	3	1	1	1	1	1	1	1
24.5	0	0	0	0	0	0	0	3	3	3	3	1	1	1	1	1	1	1	1	1
26.5	0	0	0	0	0	0	0	3	3	3	3	1	1	1	1	1	1	1	1	1
28.5	0	0	0	0	0	0	3	3	3	3	1	1	1	1	1	1	1	1	1	1
30.5	0	0	0	0	0	0	3	3	3	1	1	1	1	1	1	1	1	1	1	1
32.5	0	0	0	0	0	3	3	3	1	1	1	1	1	1	1	1	1	1	1	1
34.5	0	0	0	0	0	3	3	3	1	1	1	1	1	1	1	1	1	1	1	1
36.5	0	0	0	0	0	3	3	1	1	1	1	1	1	1	1	1	1	1	1	1
38.5	0	0	0	0	3	3	3	1	1	1	1	1	1	1	1	1	1	1	1	1
40.5	0	0	0	0	3	3	3	1	1	1	1	1	1	1	1	1	1	1	1	1
42.5	0	0	0	0	3	3	1	1	1	1	1	1	1	1	1	1	1	1	1	1
44.5	0	0	0	0	3	3	1	1	1	1	1	1	1	1	1	1	1	1	1	1
46.5	0	0	0	3	3	3	1	1	1	1	1	1	1	1	1	1	1	1	1	1
48.5	0	0	0	3	3	1	1	1	1	1	1	1	1	1	1	1	1	1	1	1
50.5	0	0	0	3	3	1	1	1	1	1	1	1	1	1	1	1	1	1	1	1
52.5	0	0	0	3	3	1	1	1	1	1	1	1	1	1	1	1	1	1	1	1
54.5	0	0	0	3	3	1	1	1	1	1	1	1	1	1	1	1	1	1	1	1
56.5	0	0	0	3	3	1	1	1	1	1	1	1	1	1	1	1	1	1	1	1
58.5	0	0	0	3	1	1	1	1	1	1	1	1	1	1	1	1	1	1	1	1
60.5	0	0	0	3	1	1	1	1	1	1	1	1	1	1	1	1	1	1	1	1
62.5	0	0	3	3	1	1	1	1	1	1	1	1	1	1	1	1	1	1	1	1

Perturbation limit tests of field voltage and phase for 0.1 % and 0.1 degree error limits:
Key: 0 = Passes both tests, 1 = Fails both tests, 2 = Fails field test, 3 = Fails phase test

Beam current in mA:	Pulse length in us:																			
	1	2	3	4	5	6	7	8	9	10	11	12	13	14	15	16	17	18	19	20
2.5	0	0	0	0	0	0	0	0	0	0	0	0	0	0	0	3	3	3	3	3
4.5	0	0	0	0	0	0	0	0	3	3	3	3	1	1	1	1	1	1	1	1
6.5	0	0	0	0	0	3	3	3	1	1	1	1	1	1	1	1	1	1	1	1
8.5	0	0	0	0	3	3	1	1	1	1	1	1	1	1	1	1	1	1	1	1
10.5	0	0	0	3	3	1	1	1	1	1	1	1	1	1	1	1	1	1	1	1
12.5	0	0	3	3	1	1	1	1	1	1	1	1	1	1	1	1	1	1	1	1
14.5	0	0	3	1	1	1	1	1	1	1	1	1	1	1	1	1	1	1	1	1
16.5	0	0	3	1	1	1	1	1	1	1	1	1	1	1	1	1	1	1	1	1
18.5	0	0	3	1	1	1	1	1	1	1	1	1	1	1	1	1	1	1	1	1
20.5	0	3	1	1	1	1	1	1	1	1	1	1	1	1	1	1	1	1	1	1
22.5	0	3	1	1	1	1	1	1	1	1	1	1	1	1	1	1	1	1	1	1
24.5	0	3	1	1	1	1	1	1	1	1	1	1	1	1	1	1	1	1	1	1
26.5	0	3	1	1	1	1	1	1	1	1	1	1	1	1	1	1	1	1	1	1
28.5	0	1	1	1	1	1	1	1	1	1	1	1	1	1	1	1	1	1	1	1
30.5	0	1	1	1	1	1	1	1	1	1	1	1	1	1	1	1	1	1	1	1
32.5	0	1	1	1	1	1	1	1	1	1	1	1	1	1	1	1	1	1	1	1
34.5	0	1	1	1	1	1	1	1	1	1	1	1	1	1	1	1	1	1	1	1
36.5	0	1	1	1	1	1	1	1	1	1	1	1	1	1	1	1	1	1	1	1
38.5	3	1	1	1	1	1	1	1	1	1	1	1	1	1	1	1	1	1	1	1
40.5	3	1	1	1	1	1	1	1	1	1	1	1	1	1	1	1	1	1	1	1
42.5	3	1	1	1	1	1	1	1	1	1	1	1	1	1	1	1	1	1	1	1
44.5	3	1	1	1	1	1	1	1	1	1	1	1	1	1	1	1	1	1	1	1
46.5	3	1	1	1	1	1	1	1	1	1	1	1	1	1	1	1	1	1	1	1
48.5	3	1	1	1	1	1	1	1	1	1	1	1	1	1	1	1	1	1	1	1
50.5	3	1	1	1	1	1	1	1	1	1	1	1	1	1	1	1	1	1	1	1
52.5	3	1	1	1	1	1	1	1	1	1	1	1	1	1	1	1	1	1	1	1
54.5	3	1	1	1	1	1	1	1	1	1	1	1	1	1	1	1	1	1	1	1
56.5	3	1	1	1	1	1	1	1	1	1	1	1	1	1	1	1	1	1	1	1
58.5	1	1	1	1	1	1	1	1	1	1	1	1	1	1	1	1	1	1	1	1
60.5	1	1	1	1	1	1	1	1	1	1	1	1	1	1	1	1	1	1	1	1
62.5	1	1	1	1	1	1	1	1	1	1	1	1	1	1	1	1	1	1	1	1

Figure 4.16: The results of the superconducting cavity perturbation simulation with a Lorentz force constant of 30.

Chapter 5

BPM model measurements

5.1 ESS BPM system parameters

The planned ESS linear accelerator BPM system is described in section 3.7 on page 14 and covered in detail in [9]. The accuracy and resolution requirements for the system are presented in table 5.1.

Table 5.1: ESS BPM accuracy and resolution requirements.

Parameter	Value [unit]
Position measurement accuracy	100 [µm]
Position measurement resolution	20 [µm]
Phase measurement accuracy	1 [degrees]
Phase measurement resolution	0.2 [degrees]

The ESS design of the spokes section BPM system calls for a beam pipe diameter of 60 mm, a button diameter of 24 mm and a button capacitance of 5.2 pF in order to work with beam currents from 6.25 mA - 62.5 mA consisting of protons traveling at 0.41 to 0.56 times the speed of light. The currents and particle speeds create bounds for the signal strength, higher particle speeds and lower currents causes lower signal strength for the BPMs.

Using the ESS BPM system design parameters from [9], see table 5.2, the expected output levels were calculated using equations (3.42) and (3.43) from section 3.9 on page 17.

Table 5.2: ESS BPM system design parameters for spoke section

Parameter	Value	Unit
f_1	352.21	MHz
f_2	704.42	MHz
Z_0	50	Ω
C_{button}	5.2	pF
r_{button}	12	mm
r_{pipe}	30	mm
β_{min}	0.41	[1]
β_{max}	0.56	[1]
$I_{beam,min}$	6.25	mA
$I_{beam,max}$	62.5	mA
$\sigma(rms)$	2.5	mm

Since both the RF feed frequencies f_1, f_2 were much smaller than the inverse of the bunch length σ the frequency dependent beam current $I_{beam}(\omega)$ could be approximated as twice the average beam current [13], i.e.

$$f_1, f_2 \ll \frac{1}{\sigma} \Rightarrow I_{beam}(\omega) \approx 2I_{beam}$$

where I_{beam} is the average beam current. According to the design [9] the cables transmitting the signal from the button BPMs in the accelerator to the measuring equipment will be approximately 60 m long. For the purpose of these calculations they were assumed to be exactly 60 m long and to have an attenuation of 4.2 dBm/100 m at 352.21 MHz and 6.2 dBm/100 m at 704.42 MHz.

The resulting signal strength bounds from the analytic modeling are presented in table 5.3. Note that the signal levels for the off-centered beam presented in table 5.3 refer to the BPM that is furthest from the beam regarding the minimum and to the BPM that is closest to the beam regarding the maximum. Also note that the signal levels for the off-centered beam are calculated using a simple model assuming a linear relation between beam displacement and signal attenuation with an attenuation of 0.5813 dB/mm. Thus the signal level for the closer BPM is increased by 8.72 dB and the signal level for the farther BPM is decreased by 8.72 dB.

Table 5.3: Expected output levels from the 60 mm BPM system [15].

Parameter	Minimum	Maximum
Centered beam		
Output level at 352.21 MHz	-27.83 dBm	-5.12 dBm
Output level at 704.42 MHz	-25.41 dBm	-2.7 dBm
Off-centered beam		
Output level at 352.21 MHz	-36.55 dBm	3.6 dBm
Output level at 704.42 MHz	-34.14 dBm	6.02 dBm

During some stages of beam commissioning the linear accelerator is unpowered from the spokes section onwards, causing the beam to de-bunch significantly in the longitudinal direction before reaching the nearest beam dump. This debunching significantly degrades signal strength and thus the BPM resolution [9]. In the worst case scenario, measuring a low current beam that is significantly debunched, the 704.42 MHz signal is expected to disappear completely while the 302.21 MHz signal is expected to be attenuated an additional 70 dB compared to the values in table 5.3 [15]. Nevertheless it is important to get at least a rough estimation of the beam position even under these conditions to successfully steer the beam to the beam dump without damaging any component of the linear accelerator. Therefore the testing includes some testing of very weak signal scenarios.

5.2 BPM test bench

The BPM test bench consists of a pipe segment with a 60 mm diameter, a thin copper wire simulating the proton beam, four BPM buttons to measure the wire position and a sliding unit that allows movement of the wire in the x-direction, see figure 5.1 for the test bench and figure 5.2 for the input orientation. The wire holding segments are connected to the pipe segment by multiple grounded metal springs to prevent field leakage from the pipe. The BPMs mounted on the test bench are somewhat smaller, measuring 16 mm in diameter rather than the 24 mm in diameter called for by the design, which likely has some negative impact on signal strength.

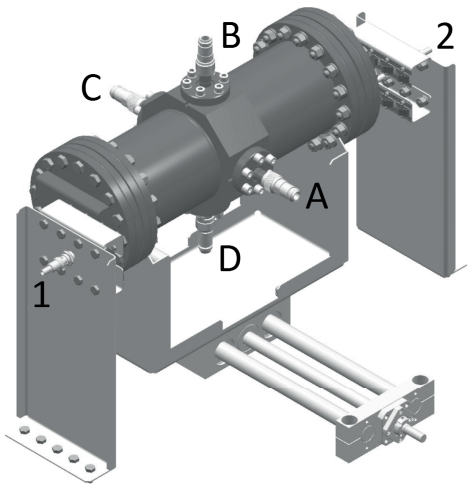

Figure 5.1: Port convention for the BPM test bench.

5.3 Measurement set up

The measurement set up is shown in figure 5.3. The RF signal created by the RF generator is split in two and routed through 300 MHz low-pass filters to attenuate undesired signals. One of the signals is routed through a phase shifter and used as a reference. The other is attenuated 20 dB to optimize the signal input level for the RF amplifier in order to reduce non-linearity contributions to the signal. It is then amplified in the RF amplifier and filtered once again before entering the BPM test bench. The four beam position monitors of the BPM test bench are connected to the LIBERA measurement unit according to the port convention in figure 5.1. An external trigger generator is used to trigger the LIBERA measurement unit.

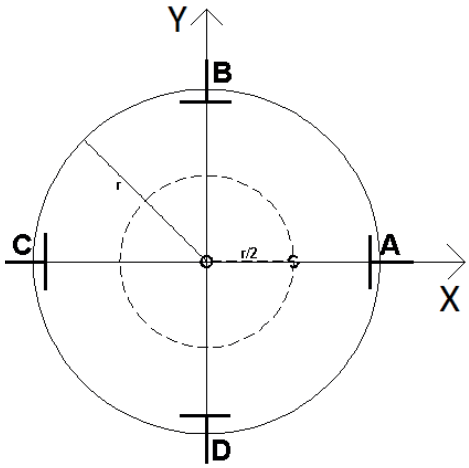

Figure 5.2: Inputs orientation for the BPM test bench, the beam direction is into the paper. The small center circle indicates a centered beam position while the small dashed off-center circle indicates the worst case scenario of an off-center beam position.

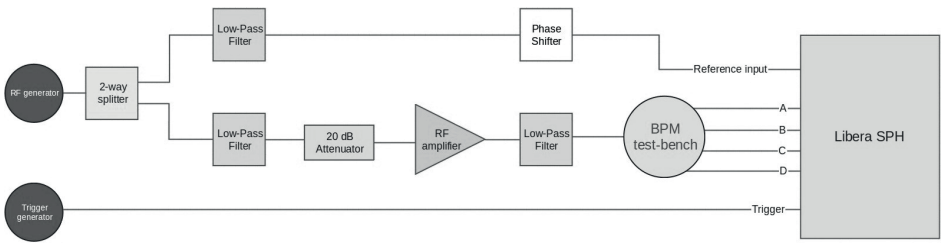

Figure 5.3: Measurement set up for BPM model measurements.

5.4 S-parameters and model adjustments

The Vector Network Analyzer, hereafter VNA, was calibrated using an electronic calibration kit and the reflection OSM (Open, Short, Match) setting of the VNA. S-parameters were measured in the 300-800 MHz range.

The return loss at the input of the BPM test bench can be determined by measuring the absolute value of the S11 parameter, see figure 5.4. At 352.21 MHz the module of S11 is -1.786 dB which corresponds to 66.3 % of the input power being reflected. At 704.42 MHz the absolute value of S11 is -1.432 dB which corresponds to 71.9 % of the input power being reflected.

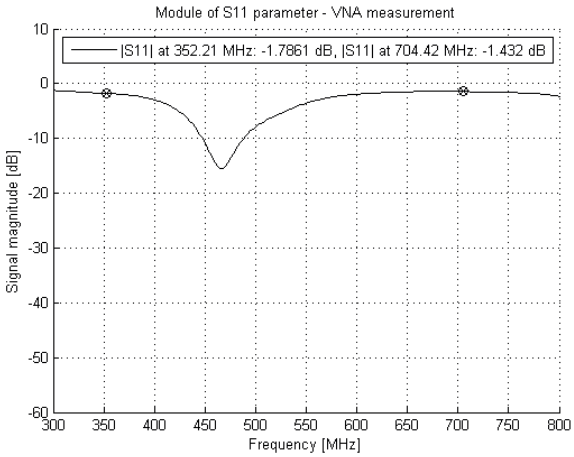

Figure 5.4: Absolute value of the S11 parameter for the BPM model.

Ideally the magnitude of the increase of the signal strength for button A when moving the wire a set distance towards it would be the same as the corresponding increase when moving the wire the same increase towards button C. As can be seen in figure 5.5 this is not the case with the measured model as there is a gap between the dashed and full lines of roughly the same magnitude.

From the measurements on button B and D in figure 5.6 there is also a noticeable gap between the dashed and full lines, implying a shift in the height of the wire as it is moved from the center.

Taken together the measurements in figure 5.5 and 5.6 show that the wire is not ideally centered in the cavity but somewhat angled, causing the asymmetry between the buttons measurements despite the same length shift from the center. Improvements to the wire holding mechanism are needed to correct these errors. Despite these errors the model can be used for the intended phase shift measurements, although with poorer precision than desired.

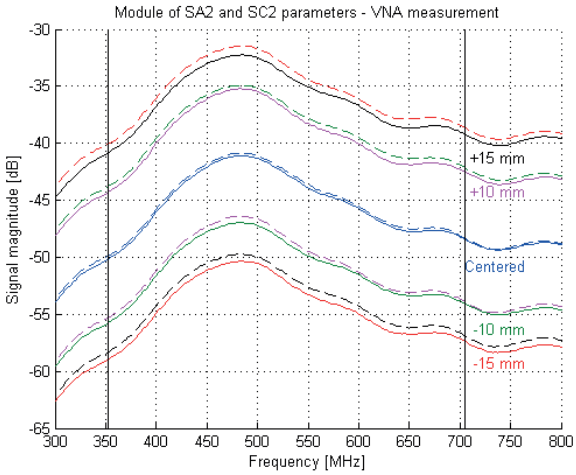

Figure 5.5: S-parameters of the BPM model, SA2 is shown in full lines and SC2 is shown in dashed lines. The frequencies of 352.21 Mhz and 704.42 Mhz are marked by black lines. Note the gap between the dashed and full lines at each level of magnitude, this implies an error in the model geometry.

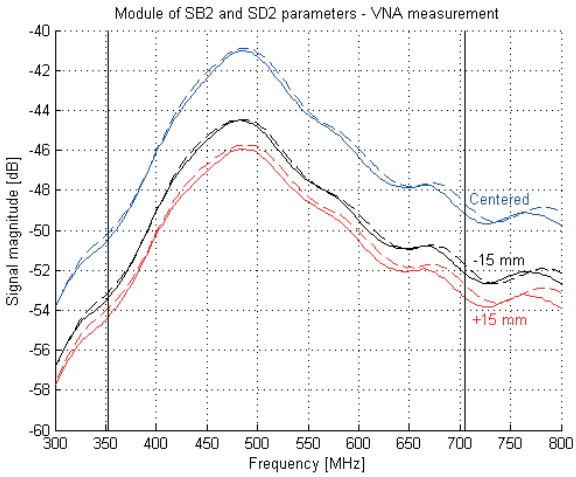

Figure 5.6: S-parameters of the BPM model, SB2 is shown in full lines and SD2 is shown in dashed lines. The frequencies of 352.21 Mhz and 704.42 Mhz are marked by black lines. Note the gap between the full and dashed lines, this implies the model is not completely symmetric.

5.5 Instrument calibration

In order to match the signal levels measured by the LIBERA unit to the wire position determined by the sliding unit of the BPM test bench calibration is necessary. The calibration procedure consists of two steps, geometric calibration and sensitivity calibration. Since the BPM test bench only allows movement in the X-direction calibration is only done for the X position.

The geometric calibration aims to compensate for any differences in signal paths from the BPMs to the LIBERA unit by introducing different gain parameters to the measured signals. Successful calibration will give read-outs of zero when the wire is centered and provide a symmetric response to wire displacement, i.e. moving the wire a set distance in the positive direction provides the same output as moving the wire the same distance in the negative direction.

Placing the wire at the center of of the pipe and running the calibration program automatically calculates the four different gain parameters necessary to even out the output signals from the BPMs. After this geometric calibration the wire position is measured across the entire measurement span, from -15 mm to +15 mm in steps of 1 mm, to determine the symmetry of the response, see figure 5.7. The linear region of the measurement span after geometric calibration was determined to -5 mm to +5 mm.

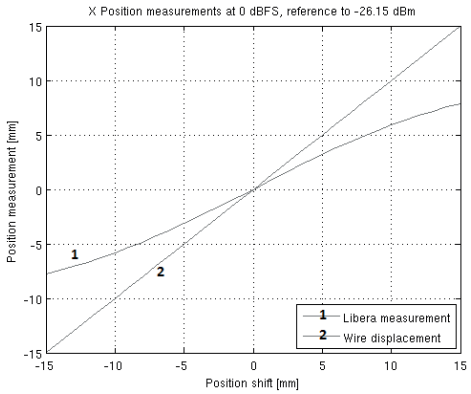

Figure 5.7: Position measurement after geometric calibration [15].

Sensitivity calibration aims to provide accurate position information in a region of the measurement span. Ideally this would be the whole span, but since the measured system is not linear this is not possible with the simple linear model used for position calculations. Sensitivity calibration is done by tuning the sensitivity coefficients, K_x, K_y, used in the position calculation formulas

$$X = K_x \frac{K_a V_a - K_c V_c}{K_a V_a + K_c V_c} \qquad Y = K_y \frac{K_b V_b - K_d V_d}{K_b V_b + K_d V_d}$$

where X,Y are the positions in the X- and Y-directions respectively, K_a, K_b, K_c, K_d are the gain parameters determined by the geometric calibration and V_a, V_b, V_c, V_d

are the voltages from the BPMs. In order to minimize errors in the linear region of the measurement span K_x is set to 15.63 while K_y is left at the default value of 10. This differs somewhat from the K_x value of 15.18 that was derived from simulations [15]. This might be because of the inexactness of the wire positioning in the BPM test bench.

5.6 LIBERA measurements

The purpose of these measurements is to analyze the limitation of BPMs in detecting the phase and position of the beam.

Measurements are performed for positions shifts of -15 mm to 15 mm in steps of 1 mm for signal strengths from -26.15 dBm to -56.15 dBm in steps of 10 dB. At -66.15 dBm the signal is indistinguishable from noise, thus the cut-off point.

The resolution of the phase and position measurements is defined as the standard deviation σ, calculated from the 2000 samples acquired within one trigger acquisition, i.e.

$$\sigma = \sqrt{\frac{1}{2000}\sum_{i=1}^{2000}(x_i - \bar{x})^2} \tag{5.1}$$

where x_i is the samples and $\bar{x}$ is the mean of the samples. The impact of the position shift on the phase resolution and position resolution is shown in figure 5.8 and figure 5.9 respectively.

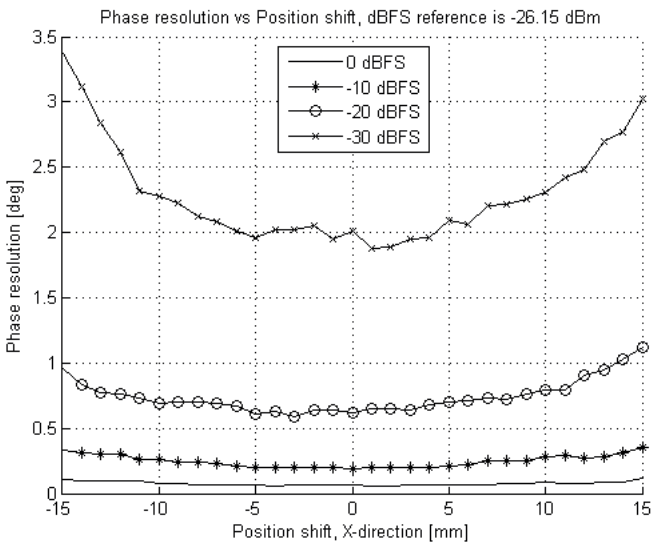

Figure 5.8: Phase resolution as a function of wire position shift.

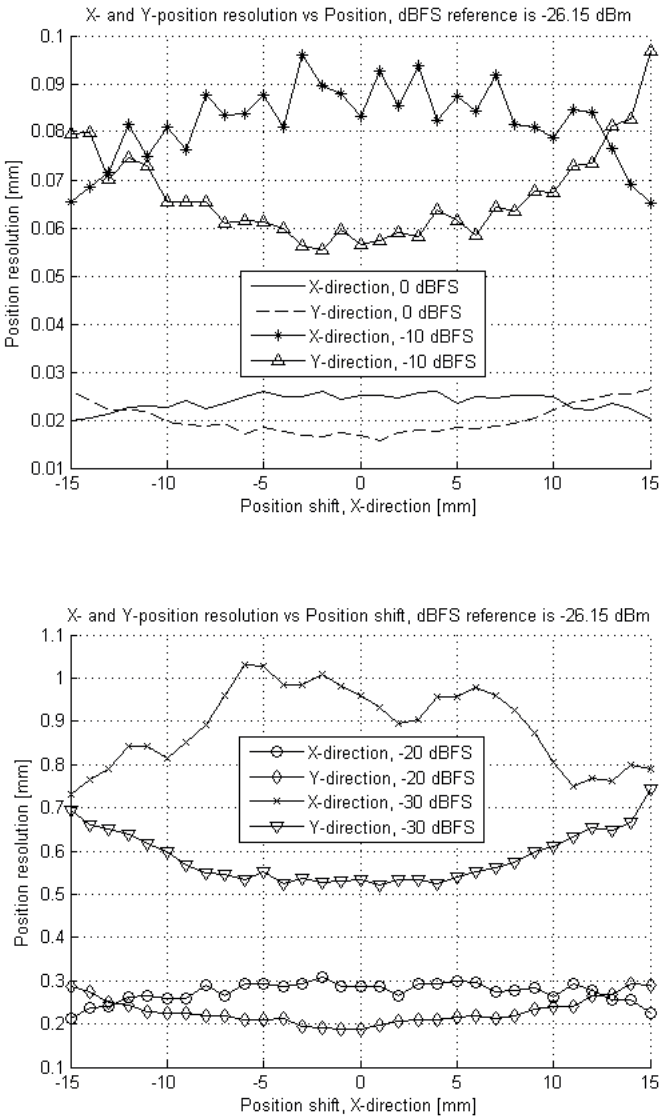

Figure 5.9: Position resolution as a function of wire position shift.

The phase resolution degrades the further the wire is from the center. This is to be expected since the phase is averaged between the four BPMs and moving it from the center increases the distance to three of them, thus degrading the signal and increasing the impact of noise. There is a noticeable gap between the X and Y position resolution measurements even when the wire is centered. This is because of the different sensitivity coefficients for X and Y applied in the sensitivity calibration, see section 5.5. The X position resolution increases the further the wire is from the center. This is because the better signal from the closer BPM outweighs the degradation of the signal from the farther BPM to the extent that the average is better than that of the two average signals provided when the wire is centered. For the Y position the resolution decreases the farther the wire is from the center since this corresponds to a longer distance to both Y-direction BPMs. Both phase and position resolutions degrades significantly with a lower signal strength. This is expected since the weaker the signal the harder it is to separate it from the noise. It does underline the importance of a high beam current for beam position monitoring however.

The accuracy of the measurements, i.e. how close the measured values are to the real values, is evaluated as the difference between the measured values and the numeric reference from the sliding unit of the BPM test bench. This introduces some error sources. The sliding unit is adjusted by a control knob with a 50 µm resolution, which is only half the resolution required by ESS at the time of writing. As the sliding unit moves the pipe section, the BPM cables are bent, which might influence the measurements. As mentioned in section 5.4 the wire positioning in the pipe is not ideal, causing some asymmetry between positive and negative position shifts.

The accuracy evaluation of the position shift is shown in figure 5.10. Since the wire position is not adjustable in the Y direction the accuracy evaluation was only performed for the X direction. Figure 5.11 shows the results of the accuracy evaluation in the linear region of the measurement span, -5 mm to +5 mm, where the sensitivity calibration has a positive effect. It is notable that only signals of -10 dBFS, i.e. -36.15 dBm, and higher meet the ESS accuracy limits.

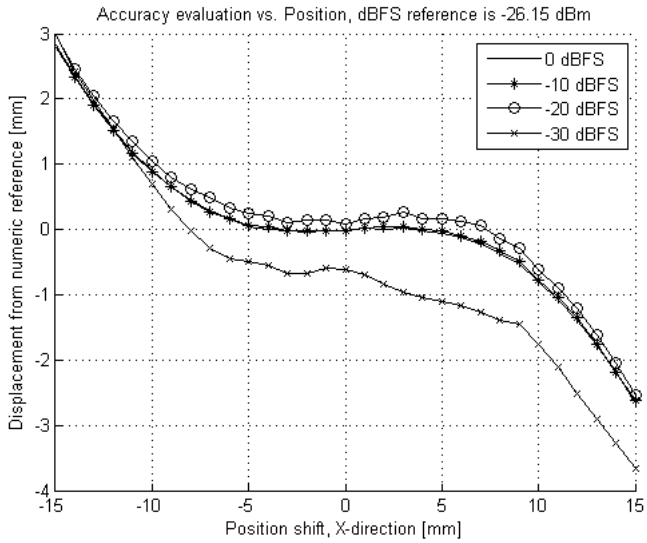

Figure 5.10: Position accuracy dependence on wire position.

The actual phase, X-position and Y-position measurements are shown in figures 5.12, 5.13 and 5.14 respectively, see pages 53-54. The problem with measuring a weak signal is especially noticeable in figure 5.14.

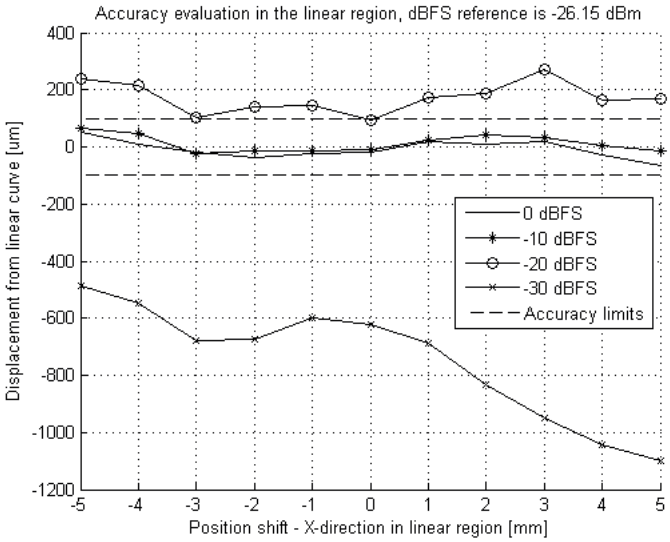

Figure 5.11: Position accuracy dependence on wire position in the linear region of the measurement range. Signal strengths of -20 dBFS and lower fail to meet the ESS accuracy limits.

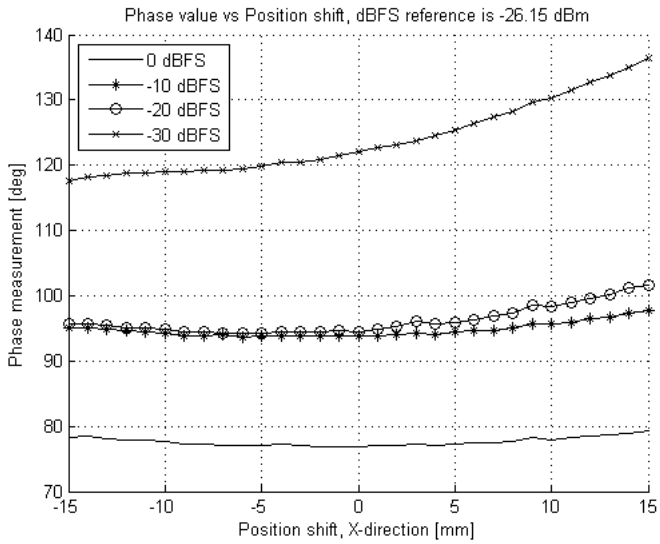

Figure 5.12: Measured phase for the BPM test bench.

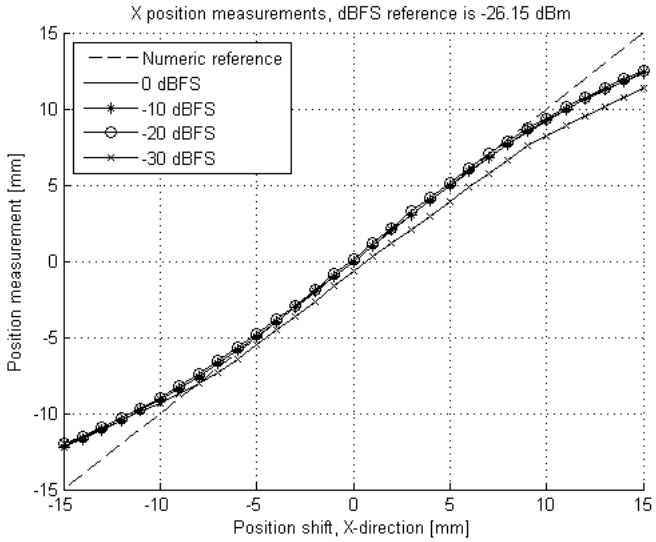

Figure 5.13: X position measurements for the BPM test bench.

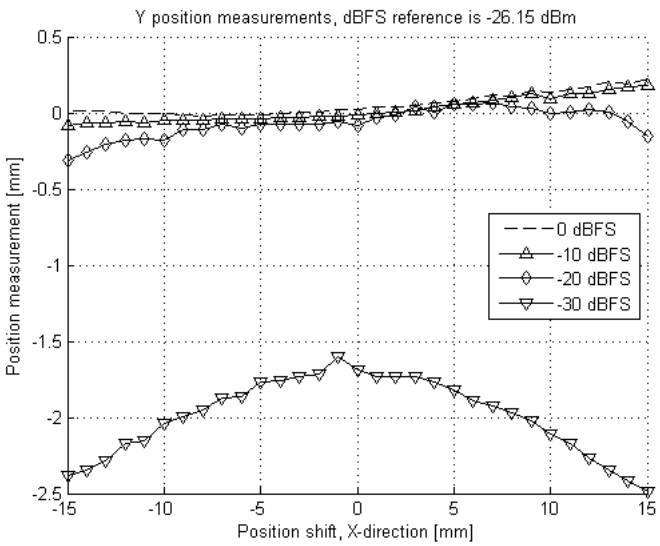

Figure 5.14: Y position measurements for the BPM test bench. Note the asymmetry between positive and negative position shifts, likely caused by non-ideal wire positioning in the BPM test bench.

Chapter 6
Conclusions

6.1 Cavity filling

If power minimization is the primary goal then a linear slope provides the best results, conserving power at a cost of longer rise times, see figure 4.9 on page 30 and table 6.1. If a short rise time is the primary goal then a well calibrated two-tiered pulse current shape is preferable.

However, as long as the rise and fall times fit into the time spacing between proton bunches their length is not a problem, so as long as this is the case a linear sloped current shape would be preferable.

Table 6.1: Cavity filling rise times

Pulse shape	Rise time [µs]
Two-step	36
Single-step	79.7
$6 - \tau$ exponential	109.5
$3 - \tau$ linear	105.2
$6 - \tau$ linear	138
$12 - \tau$ linear	210.3

6.2 Cavity perturbation results

Having no error correction at all is technically viable for all but the strictest error limit of 0.1 % voltage and 0.1° phase as long as the beam current is kept sufficiently small and the beam pulse length sufficiently short, see figure 6.1. In practice however this would put high demands on the beam chopper to produce the short pulse length as well as significantly increase the wear and tear the beam chopper is subjected to. High wear and tear means equipment has to be replaced often, causing facility downtime and extra expenses. In addition to these drawbacks low beam currents and short pulse lengths also makes it harder for the BPM to measure the beam position.

Perturbation limit tests of field voltage and phase for 1 % and 1 degree error limits:
Key: 0 = Passes both tests, 1 = Fails both tests, 2 = Fails field test, 3 = Fails phase test

Beam current	Pulse length in us:																			
in mA:	1	2	3	4	5	6	7	8	9	10	11	12	13	14	15	16	17	18	19	20
2.5	0	0	0	0	0	0	0	0	0	0	0	0	0	0	2	2	2	2	2	2
4.5	0	0	0	0	0	2	2	2	2	2	2	2	2	2	2	2	2	2	2	2
6.5	0	0	0	2	2	2	2	2	2	2	2	2	2	2	2	2	2	1	1	1
8.5	0	0	2	2	2	2	2	2	2	2	2	1	1	1	1	1	1	1	1	1
10.5	0	0	2	2	2	2	2	1	1	1	1	1	1	1	1	1	1	1	1	1
12.5	0	2	2	2	2	2	1	1	1	1	1	1	1	1	1	1	1	1	1	1
14.5	0	2	2	2	2	1	1	1	1	1	1	1	1	1	1	1	1	1	1	1
16.5	0	2	2	2	2	1	1	1	1	1	1	1	1	1	1	1	1	1	1	1
18.5	0	2	2	2	1	1	1	1	1	1	1	1	1	1	1	1	1	1	1	1
20.5	0	2	2	1	1	1	1	1	1	1	1	1	1	1	1	1	1	1	1	1
22.5	2	2	2	1	1	1	1	1	1	1	1	1	1	1	1	1	1	1	1	1

Perturbation limit tests of field voltage and phase for 0.5 % and 0.5 degree error limits:
Key: 0 = Passes both tests, 1 = Fails both tests, 2 = Fails field test, 3 = Fails phase test

Beam current	Pulse length in us:																			
in mA:	1	2	3	4	5	6	7	8	9	10	11	12	13	14	15	16	17	18	19	20
2.5	0	0	0	0	0	2	2	2	2	2	2	2	2	2	2	2	2	2	2	2
4.5	0	0	2	2	2	2	2	2	2	1	1	1	1	1	1	1	1	1	1	1
6.5	0	2	2	2	2	1	1	1	1	1	1	1	1	1	1	1	1	1	1	1
8.5	0	2	2	2	1	1	1	1	1	1	1	1	1	1	1	1	1	1	1	1
10.5	0	2	2	1	1	1	1	1	1	1	1	1	1	1	1	1	1	1	1	1
12.5	2	2	2	1	1	1	1	1	1	1	1	1	1	1	1	1	1	1	1	1

Perturbation limit tests of field voltage and phase for 0.1 % and 0.1 degree error limits:
Key: 0 = Passes both tests, 1 = Fails both tests, 2 = Fails field test, 3 = Fails phase test

Beam current	Pulse length in us:																			
in mA:	1	2	3	4	5	6	7	8	9	10	11	12	13	14	15	16	17	18	19	20
2.5	2	2	2	1	1	1	1	1	1	1	1	1	1	1	1	1	1	1	1	1
4.5	2	1	1	1	1	1	1	1	1	1	1	1	1	1	1	1	1	1	1	1
6.5	2	1	1	1	1	1	1	1	1	1	1	1	1	1	1	1	1	1	1	1

Figure 6.1: The results of the cavity perturbation simulation without feed-forward or feed-back error correction.

Applying feed-back error correction to the cavity is a clear improvement over using no error correction at all, especially in regards to the pulse length. Using a loop gain of 5 provided slightly better results than using a loop gain of 2 so the results of the latter case are omitted. The feedback does seem to add slightly to the phase error, compare the results for the strictest error limits in figure 6.2 with those in figure 6.1. While the results overall are clearly better than using no error correction the feed-back error correction still have mediocre results for the medium error limits of 0.5 % field strength and 0.5° phase, in practice limiting the beam current to 4.5 mA.

Perturbation limit tests of field voltage and phase for 1 % and 1 degree error limits:
Key: 0 = Passes both tests, 1 = Fails both tests, 2 = Fails field test, 3 = Fails phase test

Beam current in mA:	Pulse length in us: 1	2	3	4	5	6	7	8	9	10	11	12	13	14	15	16	17	18	19	20
2.5	0	0	0	0	0	0	0	0	0	0	0	0	0	0	0	0	0	0	0	0
4.5	0	0	0	0	0	0	0	0	0	0	0	0	0	0	0	0	0	0	0	0
6.5	0	0	0	0	0	0	0	0	0	0	0	0	0	0	0	0	0	0	0	0
8.5	0	0	0	0	0	0	0	0	0	0	0	0	0	0	0	0	0	0	0	0
10.5	0	0	2	2	2	2	2	2	2	2	2	2	2	2	2	2	2	2	2	2
12.5	0	2	2	2	2	2	2	2	2	2	2	2	2	2	2	2	2	2	2	2
14.5	0	2	2	2	2	2	2	2	2	2	2	2	2	2	2	2	2	2	2	2
16.5	0	2	2	2	2	2	2	2	2	2	2	2	2	2	2	2	2	2	2	2
18.5	0	2	2	2	2	2	2	2	2	2	2	2	2	2	2	2	2	2	2	2
20.5	0	2	2	2	2	2	2	2	2	2	2	2	2	2	2	2	2	2	2	2

Perturbation limit tests of field voltage and phase for 0.5 % and 0.5 degree error limits:
Key: 0 = Passes both tests, 1 = Fails both tests, 2 = Fails field test, 3 = Fails phase test

Beam current in mA:	Pulse length in us: 1	2	3	4	5	6	7	8	9	10	11	12	13	14	15	16	17	18	19	20
2.5	0	0	0	0	0	0	0	0	0	0	0	0	0	0	0	0	0	0	0	0
4.5	0	0	0	0	0	0	0	0	0	0	0	0	0	0	0	0	0	0	0	0
6.5	0	2	2	2	2	2	2	2	2	2	2	2	2	2	2	2	2	2	2	2
8.5	0	2	2	2	2	2	2	2	2	2	2	2	2	2	2	2	2	2	2	2
10.5	0	2	2	2	2	2	2	2	2	2	2	2	2	2	2	2	2	2	2	2

Perturbation limit tests of field voltage and phase for 0.1 % and 0.1 degree error limits:
Key: 0 = Passes both tests, 1 = Fails both tests, 2 = Fails field test, 3 = Fails phase test

Beam current in mA:	Pulse length in us: 1	2	3	4	5	6	7	8	9	10	11	12	13	14	15	16	17	18	19	20
2.5	1	1	1	1	1	1	1	1	1	1	1	1	1	1	1	1	1	1	1	1

Figure 6.2: The results of the cavity perturbation simulation using feed-back error correction with a loop gain of 5.

With feed-forward error correction and a matching error of 1 µs the results are significantly improved over both the case of no feed-forward/feed-back error correction and using feed-back error correction, see figure 6.3. The cavity field error also appears to be independent of the beam pulse length, giving the same error magnitude for all tested pulse lengths.

Simulations with feed-forward error correction and a matching error of just 0.1 µs show that both the cavity field strength and the cavity phase stay within the medium error limits for all tested beam currents and beam pulse lengths (results not pictured). Even under the strict limits of 0.1 % field strength and 0.1° phase all tested beam pulse lengths are viable up to beam currents of 20.5 mA. Presumably a smaller matching error would provide even better results, but such a small error is hard to achieve in practice.

Simulations using both feed-forward and feed-back error correction showed disappointing results. While the results are superior to using only feed-back error correction they are worse than using feed-forward correction alone, see figure 6.4 for a comparison at the medium error limits. Interestingly a loop gain of 5 produces worse results than a loop gain of 2, despite the better results of the higher loop gain in the pure feed-back simulations.

Using Feed-Forward table and a FFT matching error of 1us
Perturbation limit tests of field voltage and phase for 1 % and 1 degree error limits:
Key: 0 = Passes both tests, 1 = Fails both tests, 2 = Fails field test, 3 = Fails phase test

Beam current	Pulse length in us:																			
in mA:	1	2	3	4	5	6	7	8	9	10	11	12	13	14	15	16	17	18	19	20
2.5	0	0	0	0	0	0	0	0	0	0	0	0	0	0	0	0	0	0	0	0
4.5	0	0	0	0	0	0	0	0	0	0	0	0	0	0	0	0	0	0	0	0
6.5	0	0	0	0	0	0	0	0	0	0	0	0	0	0	0	0	0	0	0	0
8.5	0	0	0	0	0	0	0	0	0	0	0	0	0	0	0	0	0	0	0	0
10.5	0	0	0	0	0	0	0	0	0	0	0	0	0	0	0	0	0	0	0	0
12.5	0	0	0	0	0	0	0	0	0	0	0	0	0	0	0	0	0	0	0	0
14.5	0	0	0	0	0	0	0	0	0	0	0	0	0	0	0	0	0	0	0	0
16.5	0	0	0	0	0	0	0	0	0	0	0	0	0	0	0	0	0	0	0	0
18.5	0	0	0	0	0	0	0	0	0	0	0	0	0	0	0	0	0	0	0	0
20.5	0	0	0	0	0	0	0	0	0	0	0	0	0	0	0	0	0	0	0	0
22.5	2	2	2	2	2	2	2	2	2	2	2	2	2	2	2	2	2	2	2	2

Using Feed-Forward table and a FFT matching error of 1us
Perturbation limit tests of field voltage and phase for 0.5 % and 0.5 degree error limits:
Key: 0 = Passes both tests, 1 = Fails both tests, 2 = Fails field test, 3 = Fails phase test

Beam current	Pulse length in us:																			
in mA:	1	2	3	4	5	6	7	8	9	10	11	12	13	14	15	16	17	18	19	20
2.5	0	0	0	0	0	0	0	0	0	0	0	0	0	0	0	0	0	0	0	0
4.5	0	0	0	0	0	0	0	0	0	0	0	0	0	0	0	0	0	0	0	0
6.5	0	0	0	0	0	0	0	0	0	0	0	0	0	0	0	0	0	0	0	0
8.5	0	0	0	0	0	0	0	0	0	0	0	0	0	0	0	0	0	0	0	0
10.5	0	0	0	0	0	0	0	0	0	0	0	0	0	0	0	0	0	0	0	0
12.5	2	2	2	2	2	2	2	2	2	2	2	2	2	2	2	2	2	2	2	2

Using Feed-Forward table and a FFT matching error of 1us
Perturbation limit tests of field voltage and phase for 0.1 % and 0.1 degree error limits:
Key: 0 = Passes both tests, 1 = Fails both tests, 2 = Fails field test, 3 = Fails phase test

Beam current	Pulse length in us:																			
in mA:	1	2	3	4	5	6	7	8	9	10	11	12	13	14	15	16	17	18	19	20
2.5	2	2	2	2	2	2	2	2	2	2	2	2	2	2	2	2	2	2	2	2
4.5	2	2	2	2	2	2	2	2	2	2	2	2	2	2	2	2	2	2	2	2
6.5	2	2	2	2	2	2	2	2	2	2	2	2	2	2	2	2	2	2	2	2
8.5	1	1	1	1	1	1	1	1	1	1	1	1	1	1	1	1	1	1	1	1

Figure 6.3: The results of the cavity perturbation simulation using feed-forward error correction and a feed-forward matching error of 1 µs.

6.2.1 Cavity perturbation conclusions

The data shows that the harder error limitation is that on the cavity field strength. This holds true for all tested error correction methods.

Feed-forward error correction greatly increases the number of viable combinations of beam current and beam pulse length. Combining feed-back and feed-forward error correction does not improve on this result however, as shown in figure 6.4. Instead it introduces errors for certain combinations of beam current and phase, probably due to the time delay between measurement and cavity correction causing the cavity correction to overcompensate, introducing errors larger than those it was meant to correct.

In conclusion feed-forward error correction alone is the preferable method for error correction from among those tested. Using this method it is imperative to accurately measure the beam in the phase scan stage so the feed-forward signal has both the correct amplitude and is inserted with a very small phase error.

Using Feed-Forward table and a FFT matching error of 1us
Perturbation limit tests of field voltage and phase for 0.5 % and 0.5 degree error limits:
Key: 0 = Passes both tests, 1 = Fails both tests, 2 = Fails field test, 3 = Fails phase test

Beam current	Pulse length in us:																			
in mA:	1	2	3	4	5	6	7	8	9	10	11	12	13	14	15	16	17	18	19	20
2.5	0	0	0	0	0	0	0	0	0	0	0	0	0	0	0	0	0	0	0	0
4.5	0	0	0	0	0	0	0	0	0	0	0	0	0	0	0	0	0	0	0	0
6.5	0	0	0	0	0	0	0	0	0	0	0	0	0	0	0	0	0	0	0	0
8.5	0	0	0	0	0	0	0	0	0	0	0	0	0	0	0	0	0	0	0	0
10.5	0	0	0	0	0	0	0	0	0	0	0	0	0	0	0	0	0	0	0	0
12.5	2	2	2	2	2	2	2	2	2	2	2	2	2	2	2	2	2	2	2	2

Using Feed-Forward and feed-back, FFT matching error of 1us, loop gain of 5
Perturbation limit tests of field voltage and phase for 0.5 % and 0.5 degree error limits:
Key: 0 = Passes both tests, 1 = Fails both tests, 2 = Fails field test, 3 = Fails phase test

Beam current	Pulse length in us:																			
in mA:	1	2	3	4	5	6	7	8	9	10	11	12	13	14	15	16	17	18	19	20
2.5	0	0	0	0	0	0	0	0	0	0	0	0	0	0	0	0	0	0	0	0
4.5	0	0	0	0	0	0	0	0	0	0	0	0	0	0	0	0	0	0	0	0
6.5	0	0	2	2	2	0	0	0	0	0	0	0	0	0	0	0	0	0	0	0
8.5	0	2	2	2	2	2	0	0	0	2	2	2	2	0	0	0	0	2	2	2
10.5	0	2	2	2	2	2	0	0	0	2	2	2	2	2	0	0	0	2	2	2
12.5	2	2	2	2	2	2	2	2	2	2	2	2	2	2	2	2	2	2	2	2

Using Feed-Forward and feed-back, FFT matching error of 1us, loop gain of 2
Perturbation limit tests of field voltage and phase for 0.5 % and 0.5 degree error limits:
Key: 0 = Passes both tests, 1 = Fails both tests, 2 = Fails field test, 3 = Fails phase test

Beam current	Pulse length in us:																			
in mA:	1	2	3	4	5	6	7	8	9	10	11	12	13	14	15	16	17	18	19	20
2.5	0	0	0	0	0	0	0	0	0	0	0	0	0	0	0	0	0	0	0	0
4.5	0	0	0	0	0	0	0	0	0	0	0	0	0	0	0	0	0	0	0	0
6.5	0	0	0	0	0	0	0	0	0	0	0	0	0	0	0	0	0	0	0	0
8.5	0	0	0	0	0	0	0	0	0	0	0	0	0	0	0	0	0	0	0	0
10.5	0	0	0	2	2	2	2	2	2	2	2	2	2	2	2	2	2	2	2	2

Figure 6.4: Comparison of combined feed-back and feed-forward error correction, using a feed-forward matching error of 1 µs. The top section is using no feed-back, the middle section is using feed-back with a loop gain of 2 and the bottom section is using feed-back with a loop gain of 5.

6.3 Beam Position Monitoring

The measurements of the BPM test bench show that for ongoing operation even a beam current of 6.25 mA is sufficient to determine the beam position within the accuracy limits set by ESS. The accuracy of the BPM system improves with the signal strength, and should the accuracy requirements become stricter a higher beam current would be required to meet them.

While lower beam currents improve cavity field stability they cause significant problems for BPM measurements during beam comissioning as mentioned in section 3.8.1. Thus beam current should therefore be kept as high as possible and the pulse length kept as long as possible while still maintaining cavity field stability.

References

[1] Rihua Zeng, Anders Sunesson, Stephen Molloy, and David McGinnis. Turn on procedures for ess superconducting cavities. Technical report, ESS, 09-20 2013.

[2] Philip Jönsson. High precision rf measurement for ess cavity parameters. Master's thesis, Lund University, 2014.

[3] Thomas Schilcher. *Vector Sum Control of Accelerating Fields in Lorentz Force Detuned Superconducting Cavities*. PhD thesis, University of Hamburg, 03 1998.

[4] Thomas Weis. Interaction between rf-system, rf-cavity and beam. Technical report, DELTA, 03 2005.

[5] Steve Peggs. Technical design report. Technical report, ESS, 04 2013.

[6] Rihua Zeng. Field stability issue for normal conducting cavity under beam loading. Technical report, ESS, 04-26 2013.

[7] Rihua Zeng and Stephen Molloy. Some considerations on predetuning for superconducting cavity. Technical report, ESS, 03-09 2012.

[8] Valeri Ayvazyan, Stefan Choroba, Zheqiao Geng, Gevorg Petrosyan, Stefan Simrock, and Vladimir Vogel. Optimization of filling procedure for tesla-type cavities for klystron rf power minimization for european xfel. Kyoto, Japan, 2010. IPAC.

[9] H Hassanzadegan, A Jansson, A J.Johansson, R Zeng, K Strniša, and A Young. System overview and design considerations of the bpm system of the ess linac. Oxford, UK, 2013. IBIC.

[10] Peter Forck, Piotr Kowina, and Dmitry Liakin. Beam position monitors. In *Beam Diagnostics*, pages 187–228, Dourdan, France, 2008. CERN Accelerator School.

[11] H Hassanzadegan. A technical note on the expected ess bpm performance with button and stripline detectors. Technical report, ESS, 01 2014.

[12] E. Robert Shafer. Beam position monitoring. In *Beam Instrumentation Workshop, BIW89*, pages 26–58, Los Alamos, NM 87545, USA, 1990. American Institute of Physics.

[13] R. Smith Stephen. Beam position monitor engineering. SLAC-PUB-7244, 07 1996.

[14] ESS. Statement of work for 704 MHz, 1.5 MW pulsed power klystron. Technical report, ESS, 07 2014.

[15] Manuel Cargnelutti. Libera single pass h evaluation measurements at ess. Technical report, ESS, 04 2014.

LUND
UNIVERSITY

Series of Master's theses
Department of Electrical and Information Technology
LU/LTH-EIT 2015-440

http://www.eit.lth.se